Neurobiology of Disease 200 (2024) 106642

Contents lists available at ScienceDirect

Neurobiology of Disease

journal homepage: www.elsevier.com/locate/ynbdi

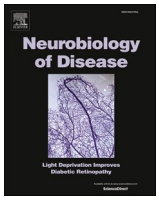

Long term effects of peripubertal stress on the thalamic reticular nucleus of female and male mice

Julia Alcaide [a,b,c,1], Yaiza Gramuntell [a,b,c,1], Patrycja Klimczak [a,b,c], Clara Bueno-Fernandez [a,b,c,2], Erica Garcia-Verellen [a], Chiara Guicciardini [a], Carmen Sandi [d], Esther Castillo-Gómez [b,e], Carlos Crespo [a], Marta Perez-Rando [a,b,c,*], Juan Nacher [a,b,c,*]

[a] Neurobiology Unit, Institute for Biotechnology and Biomedicine (BIOTECMED), Universitat de València, 46100, Spain
[b] Spanish National Network for Research in Mental Health CIBERSAM, 28029, Spain
[c] Fundación Investigación Hospital Clínico de Valencia, INCLIVA, 46010 Valencia, Spain
[d] Laboratory of Behavioral Genetics, Brain Mind Institute, Ecole Polytechnique Fédérale de Lausanne, Lausanne, Switzerland
[e] Department of Medicine, School of Medical Sciences, Universitat Jaume I, Valencia, Spain

ARTICLE INFO

Keywords:
Thalamic reticular nucleus
Peripubertal stress
Parvalbumin
Interneurons
Perineuronal nets
PSA-NCAM
NMDA receptors

ABSTRACT

Adverse experiences during infancy and adolescence have an important and enduring effect on the brain and are predisposing factors for mental disorders, particularly major depression. This impact is particularly notable in regions with protracted development, such as the prefrontal cortex. The inhibitory neurons of this cortical region are altered by peripubertal stress (PPS), particularly in female mice. In this study we have explored whether the inhibitory circuits of the thalamus are impacted by PPS in male and female mice. This diencephalic structure, as the prefrontal cortex, also completes its development during postnatal life and is affected by adverse experiences. The long-term changes induced by PPS were exclusively found in adult female mice. We have found that PPS increases depressive-like behavior and induces changes in parvalbumin-expressing (PV+) cells of the thalamic reticular nucleus (TRN). We observed reductions in the volume of the TRN, together with those of parameters related to structures/molecules that regulate the plasticity and connectivity of PV+ cells: perineuronal nets, matricellular structures surrounding PV+ neurons, and the polysialylated form of the neural cell adhesion molecule (PSA-NCAM). The expression of the GluN1, but not of GluN2C, NMDA receptor subunit was augmented in the TRN after PPS. An increase in the fluorescence intensity of PV+ puncta was also observed in the synaptic output of TRN neurons in the lateral posterior thalamic nucleus. These results demonstrate that the inhibitory circuits of the thalamus, as those of the prefrontal cortex, are vulnerable to the effects of aversive experiences during early life, particularly in females. This vulnerability is probably related to the protracted development of the TRN and might contribute to the development of psychiatric disorders.

1. Introduction

Major depression is a widespread psychiatric disorder, which affects an important part of the global population. Interestingly, major depression is more prevalent in women than in men (Kessler et al., 2003), emphasizing the importance of studies considering the gender of individuals. The fact that stress and traumatic events during early-life stages increase the prevalence of psychiatric disorders in general and particularly of major depression, is widely acknowledged (Dube et al., 2003; McKay et al., 2022). The brain retains substantial levels of neuronal plasticity well into postnatal life and some neuro-developmental events are still on course during infancy and

Abbreviations: FI, fluorescence intensity; NMDA, N-Methyl-D-Aspartate; PBS, phosphate buffered saline; PNN, perineuronal nets; PPS, peripubertal stress; PSA-NCAM, polysialylated form of the neural cell adhesion molecule; PV, parvalbumin; TRN, thalamic reticular nucleus; WFA, *Wisteria floribunda* agglutinin.

* Corresponding authors at: Neurobiology Unit, Institute for Biotechnology and Biomedicine (BIOTECMED), University of Valencia, 46100, Spain.
E-mail addresses: marta.perez-rando@uv.es (M. Perez-Rando), nacher@uv.es (J. Nacher).

[1] Julia Alcaide and Yaiza Gramuntell contributed equally to this work.

[2] *IVIRMA Global Research Alliance, IVI Foundation, Instituto de Investigación Sanitaria La Fe (IIS La Fe), Valencia, 46026, Spain. Universitat de València, Department of Pediatrics, Obstetrics and Gynaecology, Valencia, 46010, Spain.

https://doi.org/10.1016/j.nbd.2024.106642
Received 13 July 2024; Accepted 18 August 2024
Available online 22 August 2024

adolescence, particularly in some regions with protracted development, such as the prefrontal cortex (Baker et al., 2015; Shaw et al., 2020). Consequently, during this postnatal time window the neuronal circuits of these regions are particularly susceptible to the changes in structure and connectivity induced by stressful events (Malave et al., 2022; Tzanoulinou and Sandi, 2017). Numerous studies have shown the impact of early chronic stress on excitatory neurotransmission and principal cells in different brain regions (Eiland et al., 2012; Yamamuro et al., 2018), which are likely mediated, at least partially, by glucocorticoids acting on specific receptors (McEwen, 2016).

Since the physiology and synchronization of excitatory neurons is tightly controlled by GABAergic interneurons, many recent studies are focusing on the impact of early stress on the inhibitory circuitry. Indeed, the GABAergic system is not only altered by different stressors but also in patients with major depression (Fogaça and Duman, 2019; Perez-Rando et al., 2022). Among the several subpopulations of interneurons, parvalbumin (PV) -expressing interneurons are particularly susceptible to adverse experiences (Perlman et al., 2021). They are fast-spiking neurons that regulate the firing of pyramidal cells and shape brain synchronicity (Hu et al., 2014). Different studies have shown that in animal models of early chronic stress, such as maternal separation or post-weaning social isolation, PV+ cells are altered in different cerebral regions, including the prefrontal cortex (Castillo-Gómez et al., 2017; Gildawie et al., 2021; Klimczak et al., 2021).

A substantial proportion of PV+ cells is surrounded by specializations of the extracellular matrix (ECM) called perineuronal nets (PNN) (Celio et al., 1998), which limit their plasticity (Hensch, 2005), regulate their synaptic input and activity (Carceller et al., 2020), protect them from oxidative stress (Cabungcal et al., 2013) and participate in the closure of critical periods of development mediated by these inhibitory neurons ((Pizzorusso et al., 2002); see Carceller et al. (2023) for review). Different chronic stressors acting during infancy and/or adolescence have a strong impact on the PNN in different brain regions, including the medial prefrontal cortex or the hippocampus (Bueno-Fernandez et al., 2021; Castillo-Gómez et al., 2017; Murthy et al., 2019).

The structure, afferent and efferent connectivity and activity of interneurons, and particularly those of PV+ cells, are similarly regulated by the polysialylated form of the neural cell adhesion molecule (PSA-NCAM) (Nacher et al., 2013). In the cerebral cortex and other regions of the adult telencephalon, such as the amygdala, PSA-NCAM is mainly expressed in inhibitory interneurons (Nacher et al., 2002; Varea et al., 2007) and this expression is altered by chronic stress, both during adulthood (Cordero et al., 2005; Gilabert-Juan et al., 2011; Sandi et al., 2001) and during early life (Bueno-Fernandez et al., 2021; Castillo-Gómez et al., 2017; Gilabert-Juan et al., 2012).

The synaptic input of PV+ interneurons is also regulated by N-Methyl-D-Aspartate glutamate receptors (NMDAR) (Carlén et al., 2012), which are highly expressed in brain regions related with the stress response, such as the prefrontal cortex and hippocampus (Monyer et al., 1994). NMDAR are tetramers that always express the GluN1 subunit associated with a variable combination of GluN2 and GluN3 subunits (Hansen et al., 2017). Interestingly, these receptors are broadly expressed in the thalamus, particularly the GluN2C subunit (Vukadinovic, 2014). Moreover, at least in the hippocampus, they are affected by chronic stress (Sun et al., 2020) in a sex dependent manner (Hyer et al., 2021).

The excitability of PV+ cells can be regulated by glial cells (Gibel-Russo et al., 2022). Chronic stress alters the structure and physiology of glial cells, especially those of microglia and astrocytes, which may, in turn, influence the activity of PV+ interneurons (Cathomas et al., 2022). Moreover, there is evidence of the involvement of glial cells in the induction of depressive-like behaviors (Banasr and Duman, 2008), a process that may involve the interaction between glial cells and PNN (Coppola et al., 2019). In fact, there is increasing evidence of the impact of early stress on the distribution, morphology and physiology of astroglial and microglial cells (Orso et al., 2023).

Most of the studies on the effects of early stress have focused on the canonical brain areas related to stress responses: prefrontal cortex, hippocampus and amygdala. However, evidence points to a dysregulation of a medial/orbitofrontal circuit in major depression, which includes some subcortical structures such as the thalamus (Mayberg, 2003). This region is especially interesting, because it has direct connections with amygdala and the prefrontal cortex, and this connectivity is involved in the control of depressive-like behaviors (Zhao et al., 2021). Moreover, volumetric analyses in patients with major depression evidence significant structural alterations in the thalamus (Lu et al., 2016; Zhang et al., 2012). In this diencephalic region, the inhibitory control is carried out mainly by a specific GABAergic nucleus denominated thalamic reticular nucleus (TRN) (Houser et al., 1980). In this structure, thalamo-cortical and cortico-thalamic axons intersect, leaving collaterals that connect with the inhibitory neurons (Guillery and Harting, 2003; Takata, 2020). The TRN, in turn, sends axons to all the other thalamic nuclei, where they establish inhibitory synapses (Scheibel and Scheibel, 1966), which control thalamic excitability (Krol et al., 2018; Sherman, 2007). Interestingly, the TRN is composed mainly of PV-expressing neurons (Pinault, 2004) and finishes its development during postnatal life, when a progressive increase in PV expression can be detected, reflecting the final steps of the maturation of these interneurons (Frassoni et al., 1991; Majak et al., 1998). The presence of PSA-NCAM (Mazzetti et al., 2007) as well as that of PNN has been described surrounding the PV+ cells of the TRN. Particularly, PNN seem to have a fundamental role in the protection of these thalamic PV+ neurons from oxidative stress (Steullet et al., 2018). The physiology of TRN interneurons is also influenced by microglial (Liu et al., 2021) and astroglial cells (Christian and Huguenard, 2013).

There is evidence that chronic stress during adulthood influences TRN activity and its connectivity with the lateral habenula (Wang et al., 2023) and recent work from our laboratory has shown that chronic stress influences PV and PNN expression in the TRN and the habenula of adult rats (Pesarico et al., 2019). Moreover, TRN dysregulation has been described in psychiatric disorders such as schizophrenia (Cabungcal et al., 2019; Zhu et al., 2021) or major depression (Magdaleno-Madrigal et al., 2016; Velasco et al., 2006). However, there are very few studies focusing on the impact of early life stress on the thalamus and specifically on the TRN; only an electrophysiological study in rats described changes in the firing patterns of TRN neurons after maternal separation (Ali et al., 2013).

The unpredictable chronic peripubertal stress paradigm (PPS) is an excellent model of early chronic stress based on psychogenic stressors. This model induces anxiety, aggressive behaviors and attention deficits in adult male rats (Papilloud et al., 2018; Sandi, 2004; Veenit et al., 2013). Since there is strong evidence in animals (Brenhouse and Andersen, 2011; Shaw et al., 2020) and humans (Eid et al., 2019) that females are more vulnerable than males to develop stress-related disorders, we have recently used this model in male and female mice to study the effects of early chronic stress on the inhibitory networks of the medial prefrontal cortex (Bueno-Fernandez et al., 2021). We found changes in locomotion and anxiety-related behavior, the excitatory/inhibitory ratio and the complexity of the dendritic tree of PV+ neurons, as well as in the synaptic input that these cells establish on pyramidal neurons. Additionally, there were changes in the density of PSA-NCAM+ cells. Interestingly, most of the effects were observed in females.

Here, we hypothesize that PPS will alter the neuronal circuits of the thalamus by disrupting the structure and plasticity of PV+ interneurons in the TRN and that these changes will be more prevalent in female that in male mice. To test this hypothesis, we have studied how PPS affects: i) depressive-like behaviors, ii) the volume of the TRN, iii) the level of PV expression, the activation and the density of PV+ cells in the TRN, as well as the projections of these interneurons to other thalamic nuclei, iv) the density of PNN and the expression of PSA-NCAM in the TRN, v) the density of puncta expressing excitatory and inhibitory synaptic markers in the TRN, vi) the expression of NMDA receptors in PV+ cells of the

TRN and vii) the density and area covered by microglia and astrocytes in this inhibitory nucleus.

2. Material and methods

For this study, we used male and female mice from the PV-tdT line (C57BL/6-Tg(Pvalb-tdTomato)15Gfng/J (Jackson Laboratories; Bar Harbor, Maine, USA). These transgenic mice express tdTomato red fluorescent protein in PV expressing interneurons (Kaiser et al., 2016). All the experimental procedures were performed in both sexes and all the experiments were conducted in accordance with the Directive 2010/63/EU of the European Parliament and of the Council of 22 September 2010 on the protection of animals used for scientific purposes and were approved by the Committee on Bioethics of the Universitat de València. Every effort was made to minimize the number of animals used and their suffering. The animals were the same used in a previous study focused on the prefrontal cortex (Bueno-Fernandez et al., 2021).

Mice were maintained under standard housing conditions on a 12 h light-dark cycle, and food and water were available *ad libitum*. At weaning, all the mice were randomly assigned to control and PPS conditions. As previously explained, a total number of 37 PV-tdT mice were distributed in 4 groups (control female = 9, control male = 11, PPS female = 9 and PPS male = 8). It is important to note that due to lack of tissue availability, for some of the analysis the n per group was finally 6. The PPS protocol was started on postnatal day 28 (P28) and it lasted until P42 (Fig. 1), then mice were left without experimental procedures until they reached adulthood. At P84 and at P85 a splash test for anxiety-like and depression-like behavior, and an open field test for anxiety-like behavior, were respectively performed. At P90 all male mice were perfused. Female mice were perfused when they reached the diestrus phase to avoid differences due to oscillating sex hormones. All female mice were perfused in the range of P90 to P95. The phase of the estrous cycle was determined by the examination of vaginal smears. Thus, the vagina was flushed 3 to 5 times with phosphate buffered saline (PBS) and the final flush was placed on a glass slide and stained with toluidine blue. As described before (Caligioni, 2009), the proportion of leukocytes, nucleated epithelial cells and anucleated cornified cells was calculated to assess the phase of the cycle.

2.1. PPS protocol

The PPS protocol was the same as that described in previous papers from our laboratories (Bueno-Fernandez et al., 2021; Morató et al., 2022) and it was a modification of a protocol described first in rats (Márquez et al., 2013; Papilloud et al., 2018). Briefly, mice were exposed to 7 different stressors during 7 non-following days, between P28 and P42. The days of exposure to stressors were P28, P29, P30, P34, P36, P40, P42. In each day, the order and timing of the stressors were changed; consequently, an unpredictable schedule was created (Fig. 1). Stressors were applied during the light phase in 2 different sessions separated by a resting period of minimum 3 h. The stressors were: (1) 5 min exposure to a novel environment (NE), (2) 25 min exposure to the synthetic fox odor trimethylthiazoline (TMT; 9 μL; Phero Tech Inc., Canada), (3) tail puncture simulating blood collection (B), (4) 25 min exposure to an elevated platform (EP), (5) 30 min of restrain in a PVC conical tube with multiple holes (R), (6) 10 min exposure to the tail suspension test (TST) and (7) placement for 10 min in the forced swim test (FST). Control animals were handled on the same days than mice under the PPS protocol.

2.2. Behavioral analyses

The open field and splash test were performed at P84 and P85 respectively, prior to the perfusion. In the open field each mouse was placed in the center of a black opaque plexiglass covered arena (40 × 40 cm) and was left to freely explore the chamber for 10 min. Animals were video-tracked by ANY-maze software (ANY-maze video tracking system v4.98; Stoelting Europe) and we measured the following parameters: line crossings (time the animals crossed the defined zones as center and periphery) as a motor indicator, and the percentage of the time the mice spent in the periphery respect the total time as an anxiety parameter. The periphery zone was defined as the area located between 0 and 6 cm from the walls of the apparatus. Ethanol 70% was used to wipe the chamber each time prior to its use and before subsequent tests to remove any scent clues left by the previous subjects.

For the ST, each mouse was covered with a drop of sucrose and then placed in a 3000 mL beaker. Animals were left in the beaker for 5 min while being recorded. First, the latency time until the mice started grooming was determined. In addition, the number of licks to the sucrose in each minute and in the total time were measured. Ethanol 70% was used to wipe the beaker prior to its use and before subsequent tests to remove any scent clues left by the previous subjects.

Lastly, to study the possible relationship between behavioral changes (those of this study and those reported by Bueno-Fernandez et al. (2021) and TRN histological parameters, we calculated the Spearman's rho correlation coefficient (ρ).

2.3. Perfusion

All mice were deeply anesthetized with pentobarbital and then intracardially perfused with a 4% paraformaldehyde (PFA) solution. After perfusion, the brains were extracted from the skull and their hemispheres were separated and cut into 50 μm-thick coronal sections with a vibratome (Leica VT 1000E, Leica). The sections were collected in

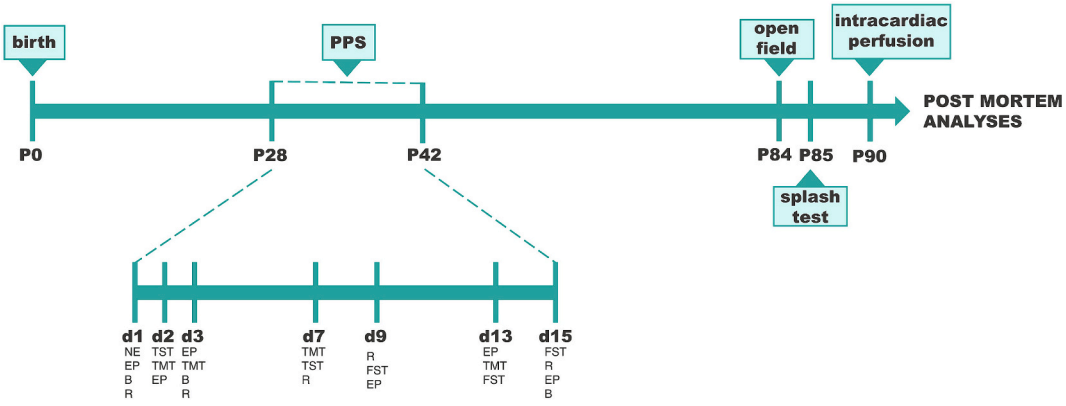

Fig. 1. Timeline of the experiment. These mice were used in a previous study (Bueno-Fernandez et al., 2021). Abbreviations: NE, novel environment; EP, elevated platform; B, Blood collection; R, restrain; TST, tail suspension test; TMT, trimethylthiazoline synthetic fox odor; FST, forced swim test.

6 subseries and stored at 4 °C in phosphate buffer (PB) 0.1 M and sodium azide 0.05% until used.

2.4. In situ hybridization analysis of NR3C1 mRNA expression in PV+ cells

In order to know whether the increase in glucocorticoids detected after PPS (Márquez et al., 2013) could directly affect PV+ neurons in the TRN, we performed an ISH RNAscope assay to study the expression of the glucocorticoid receptor (NR3C1). Prior to the assay, we perfused 3 C57BL/6-Tg(Pvalb-tdTomato)15Gfng/J control mice (P42) using 0.9% saline, extracted their brains and fixed them using PFA 4% for 24 h. After ensuring their cryoprotection, we cut them into 50 μm thick slices using a freezing-sliding microtome (Leica SM2010 R). We then started the general assay (multiplex RNAscope v2) to detect NR3C1 (MmNR3-C1 ACD #475261), PV (MmPVALB, ACD #421931-C3) and GAD1 (MmGAD1, ACD #400951-C2) mRNA. These probes were then detected using 3 different fluorophores: Opal 520 to detect GAD1 (Akoya biosciences #FP1487001KT), Opal 570 to detect NR3C1 (Akoya biosciences #FP1487001KT) and Opal 690 to detect PVALB (Akoya biosciences #FP1487001KT). Appropriate negative and positive controls were performed. After covering the samples, we imaged PV+ cells and the co-expression of glucocorticoid receptor. To do this, we performed overview single-confocal plane images using a confocal microscope (Leica TCS SPE) with a 20× magnification objective, and detailed confocal stacks using a 63× oil immersion objective with an additional digital zoom of 2.5×, and a z-step size of 0.38 μm.

2.5. Immunohistochemistry

In this study, we analyzed the expression of different molecules in the TRN using specific antibodies. Sections were washed 3 times in PBS and then incubated for 1 h in 10% normal donkey serum (NDS; Abcys) diluted in PBS with 0.2% Triton X-100 (PBST; Sigma-Aldrich). Afterward, sections were incubated with the appropriate primary antibody or *Wisteria floribunda* agglutinin (WFA) biotin-conjugated (Sigma-Aldrich) for 48 h at 4 °C (Table 1). After washing, sections were incubated for 2 h at room temperature (RT) with matching secondary antibodies or Avidin conjugated AlexaFluor-647 (Jackson Immunoresearch) (Table 1) diluted in PBST. Finally, sections were washed in phosphate buffer 0.1 M, mounted on slides and coverslipped using fluorescence mounting medium (Dako North America Inc.).

2.6. Volumetric analysis

A volumetric analysis of the TRN was performed using the PV+ cells to delimit the perimeter of the nucleus. Fifty μm-thick sections previously immunostained for PV were used. We obtained 20× microphotographs of the TRN, using a confocal microscope (Leica TCS SPE), and then processed them with the stitching plugin of FIJI-ImageJ Software (Schindelin et al., 2012), in order to have the whole nucleus on a single microphotograph. All the sections in a 1/6 subseries containing the TRN were analyzed, and the areas of the nucleus in each section were then calculated using Cavalieri's principle (Gundersen and Jensen, 1987). To obtain the volume of the nucleus, we multiplied the area by the thickness of the slice and by the number of subseries (50 μm × 6 slices), and then we did the summatory of all the slices per animal.

2.7. Immunohistochemistry image acquisition

For all the immunohistochemical analyses, except for PSA-NCAM, in each animal we took z-stacks with a 0.6 μm step size in 4 different regions of the TRN in the dorsoventral axis (Fig. 2) at bregma −1.70 mm with a confocal microscope (Leica TCS SPE). We selected the best confocal plane of each stack and processed them with a specific custom-made macro, as previously described (Guirado et al., 2018), using FIJI-ImageJ Software (Schindelin et al., 2012). Since the expression of PSA-NCAM is only particularly intense in the dorsal part of TRN, we decided to study this molecule only in this region (Fig. 2), following the same methodology described above. The specifics of each macro can be found in the supplementary material.

Table 1
Primary and secondary antibodies.

Primary antibody	Host	Dilution	Incubation	Company
Anti-PV	Guinea Pig	1: 2000	48 h, 4 °C	Synaptic Systems
Wisteria floribunda agglutinin biotin-conjugated	–	1: 200	48 h, 4 °C	Sigma-Aldrich
Anti-VGAT	Rabbit	1: 1000	48 h, 4 °C	Synaptic Systems
Anti-VGLUT1	Goat	1: 2000	48 h, 4 °C	Millipore
Anti-VGLUT2	Guinea Pig	1: 4000	48 h, 4 °C	Synaptic Systems
Anti-FosB	Mouse	1: 500	48 h, 4 °C	Abcam
Anti-PSA-NCAM	Mouse	1: 400	48 h, 4 °C	Millipore
Anti-GluN1	Rabbit	1: 400	48 h, 4 °C	Alomone
Anti-GlunN2c	Rabbit	1: 1000	48 h, 4 °C	Alomone
Anti-Iba1	Rabbit	1: 4000	48 h, 4 °C	Abcam
Anti-GFAP	Chicken	1: 8000	48 h, 4 °C	Abcam
Secondary antibody				
Anti-Guinea Pig 488	Goat	1: 400	2 h, RT	Biotium
Anti-Guinea Pig A555	Goat	1: 400	2 h, RT	Life Technologies
Avidin conjugated AlexaFluor-647	–	1: 400	2 h, RT	Jackson Life
Anti-Rabbit 488	Donkey	1: 400	2 h, RT	Technologies Life
Anti-Rabbit A647	Donkey	1: 400	2 h, RT	Technologies Life
Anti-Goat A555	Donkey	1: 400	2 h, RT	Technologies
Anti-Mouse 488	Goat	1: 400	2 h, RT	Biotium
Anti-Mouse CF647	Donkey	1: 400	2 h, RT	Biotium
Anti-Chicken CF633	Donkey	1: 400	2 h, RT	Biotium

2.8. Immunolabeling analyses

We studied 5 different parameters regarding PV and WFA immunostainings. WFA is a lectin that recognizes specifically the *N*-acetylgalactosamine moiety of chondroitin sulfate glycosaminoglycans in the PNN and it is widely used as a marker for these ECM structures, which surround PV+ cells in the TRN. We analyzed the individual fluorescence intensity (FI) of PV+ somata, the area covered by PV+ structures and the density of PV+ somata in the TRN. We also quantified the total FI of WFA in the TRN and the FI of each individual PNN. Finally, we analyzed the PV FI / PNN FI ratio, because in a previous study in the prefrontal cortex (Carceller et al., 2020) we observed a clear positive correlation between the intensities of PV and WFA immunolabelings.To study whether the inhibitory output from the TRN was affected by PPS, we analyzed the area, density and FI of the PV+ immunoreactive puncta in the lateral posterior (LP) nucleus of the thalamus, which is apposed to the TRN. In the TRN neuropil, we calculated the area, density and intensity of puncta expressing the vesicular GABA transporter (VGAT, a marker of inhibitory synapses), vesicular glutamate transporter 1 (VGLUT1, a marker of excitatory synapses of cortical origin) and the vesicular glutamate transporter 2 (VGLUT2, a marker of excitatory synapses of extracortical origin). Then, we used the densities of VGLUT1+ and VGAT+ puncta to calculate the VGLUT1/VGAT ratio. We evaluated PSA-NCAM expression analyzing the area, density and FI of PSA-NCAM+ puncta. To test whether PPS induced changes in the basal activity of TRN cells, we performed a double immunohistochemistry for PV and FosB and then measured the density of FosB+ cells and the intensity of their labeling, as well as the

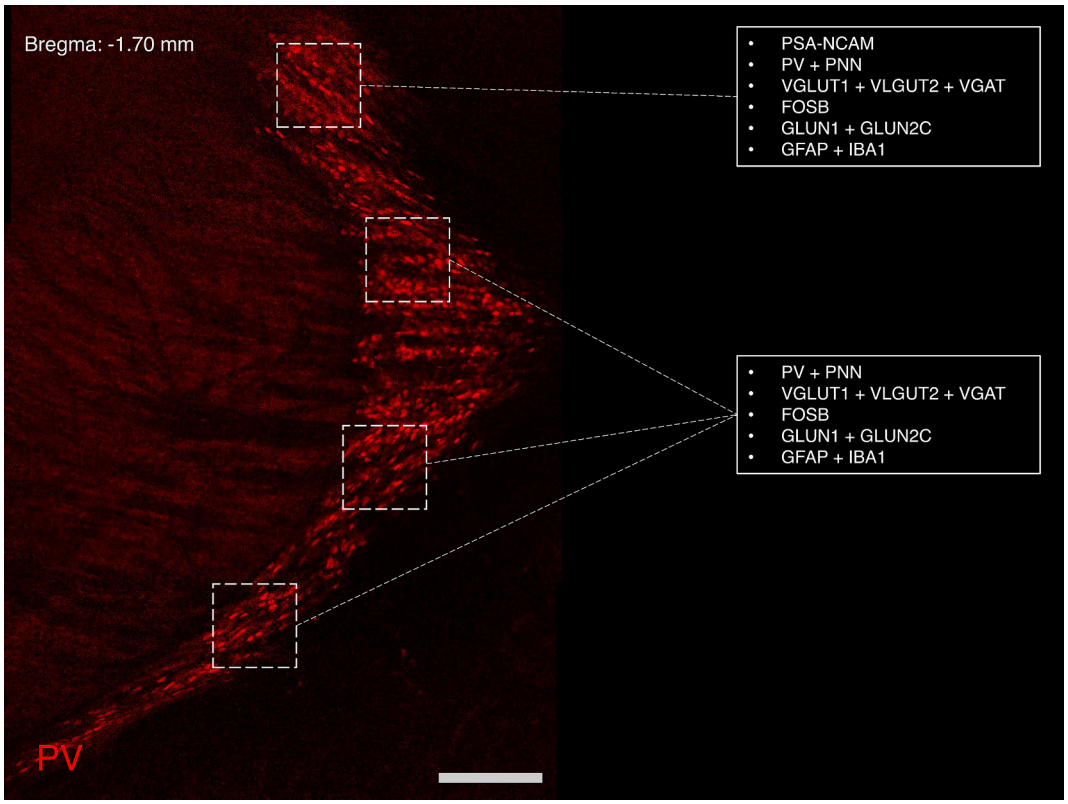

Fig. 2. Panoramic image of the murine TRN immunostained for PV. Dotted squares indicate the ROIs used for the immunofluorescence analysis. Plain squares list the molecules/structures analyzed in each region. Scale bar 200 μm.

density of FosB+PV+ interneurons. FosB is a good marker of neuronal basal activity, since it accumulates in the nucleus after repeated stimulation due to the high stability of its protein (Nestler, 2015). Next, we analyzed the expression of the GluN1 and GluN2c subunits of the NMDA receptor on PV expressing interneurons in the TRN. We calculated the FI of the structures expressing these subunits, their density, and the percentage of area covered by them. Finally, we analyzed whether PPS induced changes in TRN glial cells. Since the GFAP antibody only labels the processes, but not the somata, of astroglial cells, we only calculated the FI and the percentage of area covered by GFAP+ structures. For IBA1 we studied the density of cells, as well as the percentage of area covered by IBA1+ structures and their IF.

2.9. Statistics

The experimental design and statistical analysis were based on the indications of Diester and collaborators (Diester et al., 2019). We first analyzed pooled data from both sexes and then we segregated the data by sex and analyzed it separately. However, we decided not to analyze sex as a between-subjects factor since the determination of differences between sexes was not an objective of our study. All slides were coded prior to quantitative analysis, and the code was not broken until the quantification was completed. For all the statistical analyses, we checked the homoscedasticity and the normality of the data, and the mean ± SEM was determined. We performed unpaired Student's *t*-test analysis when there was normality and homogeneity of variances, Mann-Whitney test when the normality of the data was not achieved and a t-test with Welch's correction for the cases in which there was no homogeneity of variances. For correlations, we calculated the Spearman's rho correlation coefficient (ρ). Finally, we calculated the effect size for the *t*-tests analyses (Supplementary Table 1). We calculated Cohen's d for the analyses that had the same sample size in both groups and Hedges' G for the analyses with different sample sizes. All statistical analyses were performed using SPSS v26 (IBM, USA) or GraphPad Prism 9 (GraphPad software Inc., USA). Graphs were generated using GraphPad Prism 9. For t-tests, probability values below 0.05 were considered as statistically significant.

3. Results

3.1. Behavioral analyses

With this study we wanted to assess whether chronic variable stress during adolescence affected the behavior of adult mice. We analyzed different parameters of the open field and the splash tests performed at postnatal days 84 and 85 respectively. In the open field, we counted the number of times the mice crossed between the center and periphery areas and the percentage of time that the animals spent in the periphery. We did not find significant differences between controls and PPS mice in the analyses of these parameters (Fig. 3A-B, Table 2).

In the splash test we analyzed the latency time until mice started licking the glucose and the number of licks. There were no differences in the latency time when comparing PPS and control mice (Fig. 3C; Table 2). However, we found a significant reduction of the number of licks in the PPS mice (Fig. 3D1; Table 2) in minute 2 ($t = 2.310$, $p = 0.0285$) and tendencies towards a reduction in minute 3 and the total time when analyzing all the animals together. Additionally, there was a significant reduction of the number of licks in minutes 2 ($t = 2.171$, $p = 0.045$) and 3 ($t = 2.831$, $p = 0.013$) in females (Fig. 3D2, Table 2), while in males we only observed a trend towards a reduction of this number in the total 5 min time (Fig. 3D3, Table 2).

3.2. PPS induces a reduction of the volume of the TRN in adult female mice

To test whether there were general structural changes in the TRN

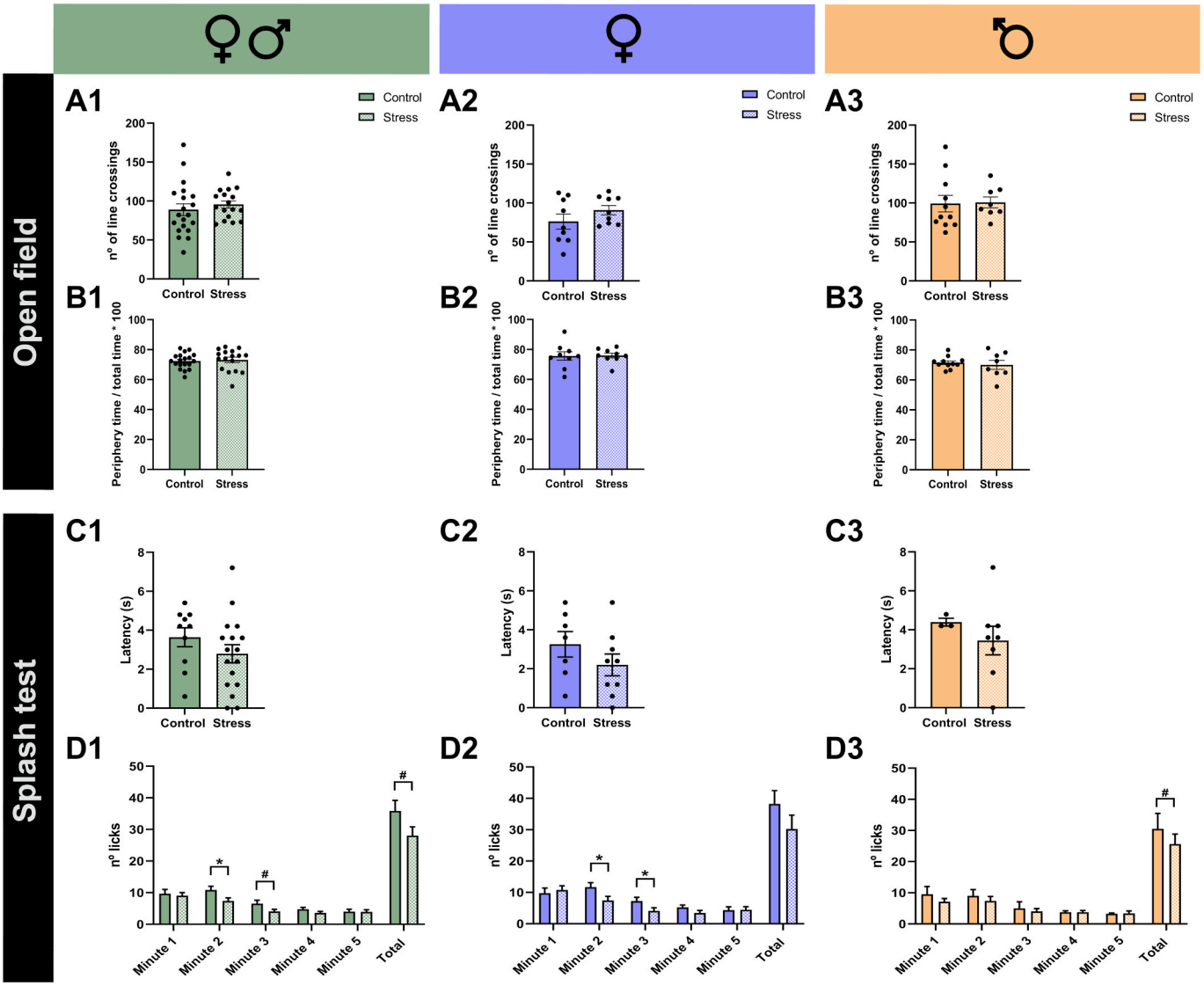

Fig. 3. Effects of the PPS model (Bueno-Fernandez et al., 2021) on the behavior of adult mice. Histograms representing the impact in the adulthood of the PPS model on the behavior of all experimental animals (not separated by sex; A1-D1), females (A2-D2) and males (A3-D3). (A) number of line crossings and percentage of time mice spent in the periphery (B) of the OF test and latency (C) and number of licks (D) 5 min after the ST. Asterisks indicate statistically significant effects of the PPS model (*$p < 0.05$).

Table 2
Summary of the behavioral results. Table summarizing the results from the behavioral tests after the PPS model. Asterisks indicate statistically significant effects of the PPS model (#0.10 ≥ p ≥ 0.05, *p < 0.05; **p < 0.01, ***p < 0.001).

	Pooled	Females	Males
Open field			
N° lines crossings	0.454	0.211	0.911
% time spent in the periphery	0.715	0.924	0.658
Splash test			
Latency	0.265	0.236	0.188
N° licks 1 min	0.689	0.640	0.314
N° licks 2 min	0.029*	0.045*	0.527
N° licks 3 min	0.062#	0.013*	0.620
N° licks 4 min	0.118	0.136	1.000
N° licks 5 min	0.941	0.941	0.917
N° licks total time	0.082#	0.211	0.097#

after the PPS protocol, we studied the volume of this thalamic nucleus. The volumetric analysis did not render significant results when pooling all animals together (Fig. 4A; Table 3). By contrast, we found a strong and significant reduction of the TRN volume specifically in females when comparing stressed *vs* control mice (Fig. 4B; Table 3; $t = 4.173$, $p = 0.001$). We found no significant differences regarding male mice (Fig. 5C; Table 3).

3.3. PPS increases the intensity of fluorescence of WFA-labeled PNN in the TRN of adult female mice but does not change parameters related to PV expression

Since many of the cells in the TRN are PV expressing neurons, which are densely surrounded by PNN, we decided to study different parameters of these inhibitory neurons and their PNN coverage. First, we studied the density of PV immunoreactive somata, the area covered by PV immunoreactivity and the intensity of PV immunofluorescence (Fig. 5A & B). None of these parameters related to PV expression was significantly different when comparing control *vs* PPS mice (Fig. 5C1-3, D1-3, E1-3; Table 3). All PV+ neurons in the TRN were surrounded by

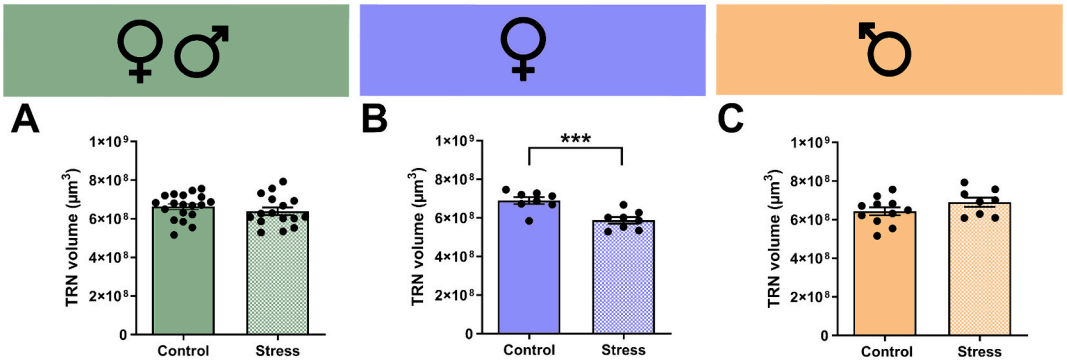

Fig. 4. Effect of the PPS model on the volume of the TRN. Histograms representing the effect of the PPS model in all animals (not separated by sex) (A), females (B) and males (C). Asterisks indicate statistically significant effects of the PPS model (***$p < 0.001$).

WFA+ PNN. We analyzed the FI of WFA in individual PNN, as well as the general WFA FI in different regions of interest inside the TRN (see Fig. 2 and material and methods section). In addition, we analyzed the ratio of PV and WFA FI. We did not find any significant change in these parameters when all the animals were pooled together (Fig. 6C4-6; Table 3), although, a trend towards an increase was observed in the PV/WFA FI ratio (Fig. 5C7; Table 3, $p = 0.074$). In females, we did not observe significant changes in the FI of individual PNN (Fig. 6D5; Table 3) but noted an increase of the general WFA FI (Fig. 5D6; Table 3; $t = 2.209$, $p = 0.043$). In the same direction, there was a significant reduction of the PV FI / PNN FI ratio (Fig. 5D7; Table 3; $t = 3.354$, $p = 0.005$). We did not find any significant change in these parameters in male mice (Fig. 5E1-7).

3.4. Male mice subjected to PPS show a reduction of FI in the puncta expressing inhibitory synaptic markers in the TRN

We next studied the excitatory (cortical and extracortical) and inhibitory synaptic input on the TRN using immunohistochemistry for the vesicular glutamate transporters 1 (VGLUT1) and 2 (VGLUT2) and the vesicular GABA transporter (VGAT) (Supplementary Figs. 2 & 3). We studied the area of individual puncta, their density, fluorescence intensity and percentage of area occupied by VGAT, VGLUT1 and VGLUT2 immunoreactive puncta. Additionally, we measured the ratio of the density of VGLUT1/VGAT immunoreactive puncta. We only found a significant decrease induced by PPS in the FI of VGAT+ puncta in male mice (Supplementary Fig. 2; Table 3; $t = 2.141$, $p = 0.032$). No significant changes were observed in the area of VGAT+ puncta, their density, FI or the area covered by them, neither in males, nor in females or in pooled animals (Supplementary Fig. 2; Table 3). Similarly, no differences were observed in these parameters in VGLUT1+ puncta or in the ratio VGLUT1/VGAT density (Supplementary Fig. 2; Table 3).

3.5. PPS does not change FosB expression in the TRN

To study whether there were long term changes in the activity of TRN neurons after the PPS protocol, we analyzed FosB expression in this nucleus. We did not find significant differences in the density of FosB positive cells in the TRN or their FI. We focused then our analysis in FosB expression on PV+ cells, but also failed to find significant differences (Supplementary Fig. 4; Table 3).

3.6. PPS induces a decrease in the density of PSA-NCAM immunoreactive puncta in the TRN of adult female mice

We next focused on studying the expression of the plasticity-related molecule PSA-NCAM. This molecule was intensely expressed in the most dorsal region of the TRN and in thin bands limiting its lateral and medial regions. The analysis of the dorsal region (Fig. 6A & B) did not reveal significant differences in the parameters analyzed when considering all animals together (Fig. 6C1-3; Table 3). In female mice, no significant differences existed in the area covered by PSA-NCAM immunoreactivity (Fig. 6D1; Table 3); however, we found a significant decrease in the density of PSA-NCAM immunoreactive puncta (Fig. 6D2; Table 3, $t = 2.474$, $p = 0.033$) and a trend towards a decrease in their FI (Fig. 6D3; Table 3; $t = 2.125$; $p = 0.063$). No significant differences were found in males (Fig. 6E1-3; Table 3).

3.7. PPS increases the density of GluN1 receptors in PV expressing neurons in the TRN of adult female mice

To study whether the PPS model affects NMDA receptors in PV+ cells, we studied the expression of GluN1 and GluN2C subunits, both broadly expressed in the TRN. Our analysis of the expression of the GluN1 subunit of the NMDA receptor in PV expressing interneurons of the TRN (Fig. 7A & B) did not reveal significant changes in any of the parameters analyzed when the animals were not separated by sex (Fig. 7C1-3; Table 3). By contrast, we observed a significant increase in the density of GluN1 immunoreactive puncta in stressed females when compared to controls (Fig. 7D1; Table 3; $t = 2.378$, $p = 0.041$). No differences were found in the other parameters analyzed in females (Fig. 7D2-3; Table 3) or when only males were studied (Fig. 7E1-3; Table 3). The analysis of the expression of the GluN2C subunit did not reveal significant changes between stressed and control mice in any of the parameters analyzed (Supplementary Fig. 5; Table 3).

3.8. Lack of PPS-induced changes in the glial cells of the TRN

Since the physiology of the TRN is strongly influenced by microglial and astroglial cells, we decided to analyze different parameters related to these glial cells in the TRN, using IBA1 and GFAP immunohistochemistry. We did not observe significant alterations in the FI, the percentage of area covered by, or the density of IBA1+ or GFAP+ cells (Supplementary Fig. 6; Table 3).

3.9. PPS induces an increase of the FI of PV immunoreactive puncta in LP nucleus of the thalamus in adult female mice

In addition, we decided to asses possible changes in the synaptic output of PV+ neurons in the TRN by analyzing PV+ puncta in the LP thalamic nucleus. After studying the PV+ puncta in this excitatory nucleus of the thalamus (Fig. 8A & B), we did not find significant differences in the area covered by PV+ puncta, their density or their FI when all animals were pooled together (Fig. 8C1-3; Table 3). By contrast, we observed a significant increase in the FI of PV+ puncta, but not in the other parameters, in adult females subjected to PPS (Fig. 8D; Table 3; $t = 1.466$, $p = 0.036$). No significant differences were found when studying male mice.

Table 3
Summary of the histological results. Table summarizing the results from the analysis performed in the TRN after the PPS model. Asterisks indicate statistically significant effects of the PPS model (#0.10 ≥ p ≥ 0.05, *p < 0.05; **p < 0.01, ***p < 0.001).

	Pooled	Females	Males
Volumetry			
Volumetry	0.328	0.001***	0.168
PV			
Area of PV immunoreactivity	0.491	0.327	0.841
Density of PV+ cells	0.568	0.182	0.931
PV FI	0.904	0.677	0.221
PNN			
WFA FI in individual PNN	0.904	0.218	0.495
WFA FI in TRN	0.958	0.043*	0.222
PV and PNN			
PV/PNN FI ratio	0.074#	0.005**	0.680
% PV + PNN+ cells	0.987	0.028*	0.474
VGAT			
Area of VGAT+ puncta	0.353	0.813	0.221
Density of VGAT+ puncta	0.790	0.787	0.981
FI of VGAT+ puncta	0.290	0.840	0.032*
% Area covered by VGAT+ puncta	0.551	0.779	0.124
VGLUT1			
Area of VGLUT1+ puncta	0.660	0.840	0.967
Density of VGLUT1+ puncta	0.847	0.373	0.430
FI of VGLUT1+ puncta	0.572	0.959	0.105
% Area covered by VGLUT1+ puncta	0.722	0.644	0.811
VGLUT1 / VGAT			
Density of VGLUT1+ puncta / Density of VGAT+ puncta * 100	0.347	0.308	0.645
VGLUT2			
Area of VGLUT2+ puncta	0.727	0.971	0.256
Density of VGLUT2+ puncta	0.874	0.674	0.394
FI of VGLUT2+ puncta	0.490	0.903	0.136
% Area covered by VGLUT2+ puncta	0.518	0.856	0.340
FosB			
Density of FosB+ cells	0.883	0.355	0.402
FI of FosB	0.834	0.571	0.665
Density of PV + FosB+ cells	0.157	0.238	0.222
PSA-NCAM			
Area of PSA-NCAM+ puncta	0.300	0.450	0.428
Density of PSA-NCAM+ puncta	0.998	0.063	0.567
FI of PSA-NCAM+ puncta	0.112	0.033*	0.680
GluN1			
Density of GluN1+ puncta	0.263	0.041*	0.153
FI of GluN1+ puncta	0.323	0.226	0.975
% Area covered by GluN1+ puncta	0.238	0.260	0.697
GluN2c			
Density of GluN2c + puncta	0.475	0.269	0.680
FI of GluN2c + puncta	0.855	0.937	0.178
% Area covered by GluN2c + puncta	0.491	0.817	0.189
GFAP			
FI of GFAP	0.114	0.264	0.323
% Area covered by GFAP	0.146	0.267	0.406
Iba-1			
Density of Iba-1+ cells	0.866	0.477	0.520
FI of Iba-1	0.656	0.588	0.984
% Area covered by Iba-1 immunoreactivity	0.523	0.605	0.729
PV puncta in LP			
Area of PV+ puncta	0.804	0.659	0.883
Density of PV+ puncta	0.852	0.990	0.897
FI of PV+ puncta	0.374	0.036*	0.769

3.10. Correlations between behavioral and histological parameters

Finally, we wanted to study whether there were correlations between the results of the behavioral analyses we performed, as well as those from Bueno-Fernandez et al. (2021) report, and the histological parameters we studied in the TRN. We found a significative negative correlation in PPS mice between the TRN volume and the number of immobile episodes in male mice (Table 4; $\rho = -0.786$; $p = 0.021$) but not in the pooled or female mice. We also observed significant negative correlations for female control mice between the WFA FI in the TRN and the n° of immobile episodes (Table 4; $\rho = -0.728$; $p = 0.037$) and n° of line crossings (Table 4; $\rho = -0.728$; $p = 0.037$) but not in pooled and male animals. Moreover, in control mice, we found significant negative correlations for female animals between the PV / PNN FI ratio and the n° of immobile episodes (Table 4; $\rho = 0.905$, $p = 0.02$) and the n° of line crossings (Table 4; $\rho = 0.929$; $p = 0.001$). For the pooled and male mice we did not find significant correlations between the PV / PNN FI ratio and the n° of immobile episodes, while there was a trend towards a negative correlation in pooled animals, but not in male mice, between the PV / PNN FI ratio and the n° of line crossings (Table 4). Also in control mice, there was a positive correlation between the density of GluN1+ puncta and the n° of line crossings in pooled animals (Table 4; $\rho = 0.7$; $p = 0.016$) and female mice (Table 4; $\rho = 0.9$; $p = 0.037$), but not in males (Table 4). In addition, we found a positive correlation between the FI of the PV+ puncta in the LP thalamic nucleus in pooled animals (Table 4; $\rho = 0667$; $p = 0.025$), while there was a negative correlation in these parameters in male mice (Table 4; $\rho = -0.928$; $p = 0.008$), but not in female mice (Table 4). Finally, there was a negative correlation between the FI of the PV+ puncta in the LP thalamic nucleus and the ratio of periphery distance / center distance in female mice (Table 4; $\rho = -0.9$; $p = 0.037$), but not in pooled or male mice (Table 4).

4. Discussion

Adverse experiences, such as stress or fear, during the first stages of life (infancy and adolescence), are known predisposing factors for certain psychiatric disorders, including major depression (Dube et al., 2003; McKay et al., 2022). These adverse experiences probably interfere with the last developmental stages of certain brain regions, which expand well into postnatal life. Such is the case of the prefrontal cortex, one of the most studied regions in this regard, but this protracted postnatal development also occurs in some other areas of the central nervous system. One of these structures is the thalamus (Alex et al., 2024), and inside it particularly the TRN, which provides intrinsic inhibitory control (De Biasi et al., 1996; Fitzgibbon, 2007; Frassoni et al., 1991; Fujita et al., 2022; Majak et al., 1998). In the present study, we have subjected male and female mice to a peripubertal stress protocol to explore long-term alterations in the structure, connectivity and plasticity of the TRN, particularly of its PV+ neurons.

The literature describing the impact of early life adverse experiences on the thalamus is still scarce and consists only of studies with stressors applied earlier than our PPS protocol. There are reports describing reduced activity in the anterior thalamus of adult rats submitted to maternal separation (P1-P21) (Banqueri et al., 2018, 2021) and it was found that sleep deprivation in kittens (P42-P49) reduced the number of

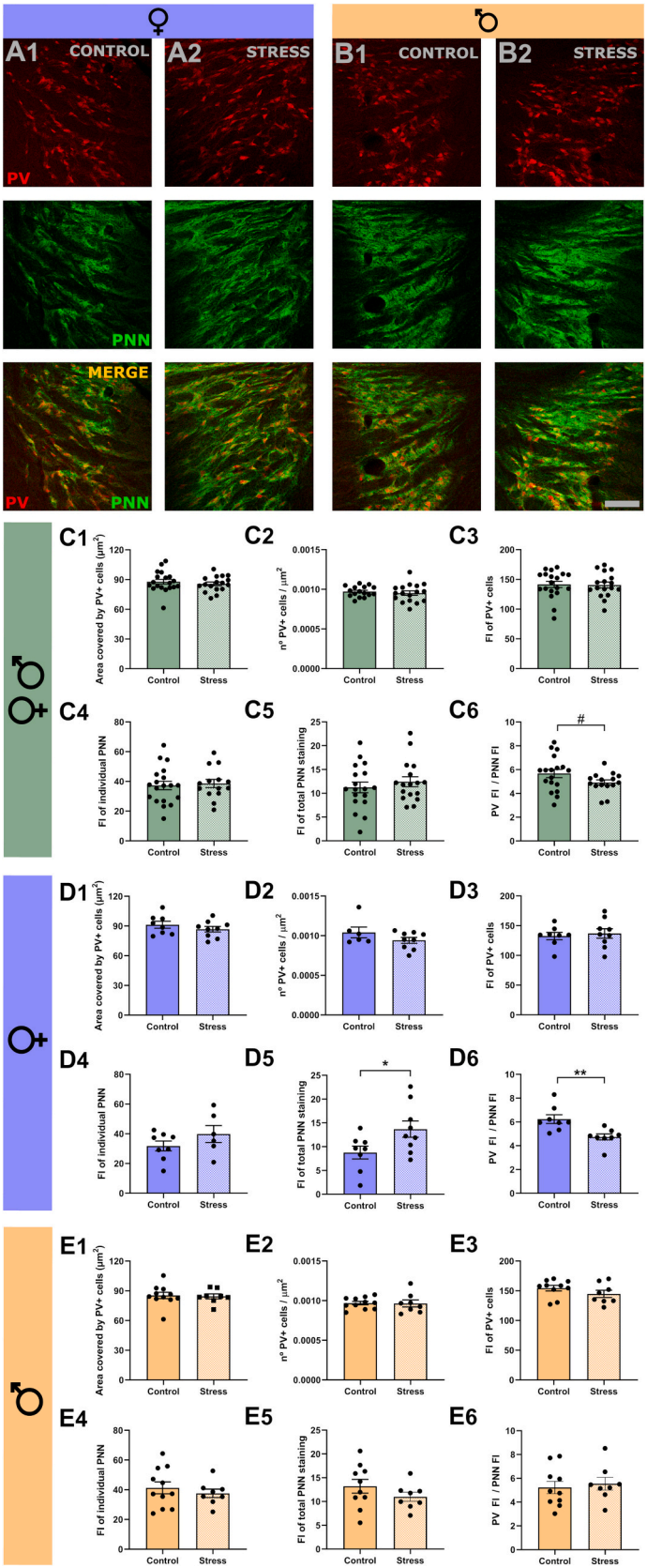

(caption on next page)

Fig. 5. Analysis of the effects of the PPS model on PV expressing cells and WFA-labeled PNN. (A-B) Representative images (single confocal planes) of PV immunoreactive cells (red), PNN labeled with *Wisteria floribunda* lectin (green) and their merged images in the TRN of adult female (A) and male (B) mice in the control (A1, B1) and stressed (A2, B2) groups. (C-E) Histograms representing the effects of the PPS model on the area covered by PV+ cells (C1, D1 & E1), the density of PV+ somata (C2, D2 & E2), the total FI of PV+ cells (C3, D3 & E3), the FI of individual PNN (C4, D4 & E4), the total FI of PNN (C5, D5 & E5), and the ratio of PV/PNN FI (C6, D6 & E6) in all animals (not separated by sex) (C), females (D) and males (E). Asterisks indicate statistically significant effects of the PPS model (**$p < 0.01$, *$p < 0.05$, #$0.1 > p > 0.05$). Scale bar 50 μm. (For interpretation of the references to colour in this figure legend, the reader is referred to the web version of this article.)

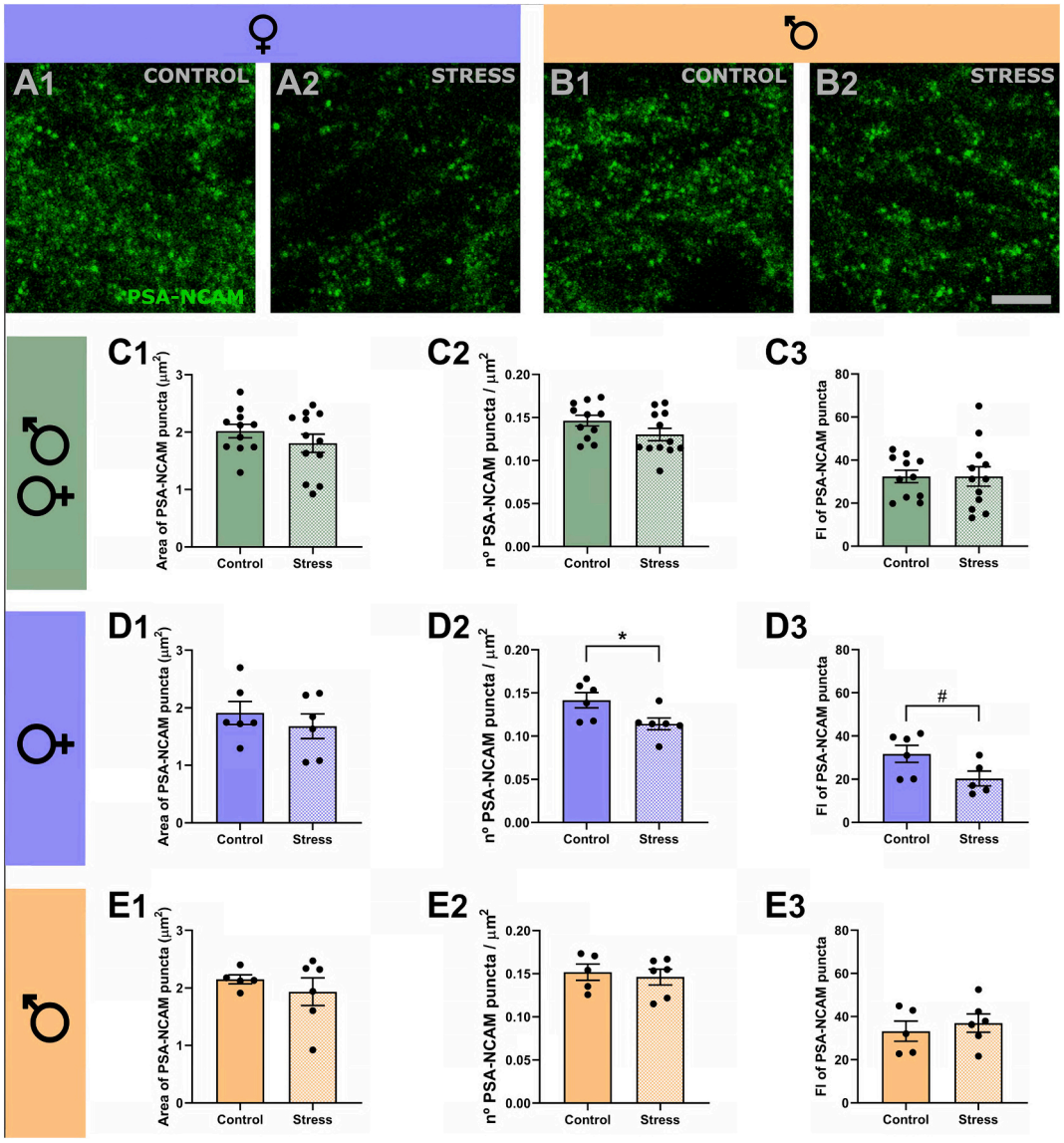

Fig. 6. Analysis of the effects of the PPS model on PSA-NCAM expression in the TRN. (A-B) Single confocal planes showing PSA-NCAM positive puncta in females (A) and males (B), comparing control mice (A1, B1) and mice that underwent PPS (A2, B2). Histograms representing differences in the area covered by PSA-NCAM+ puncta (C1, D1 & E1), their density (C2, D2 & E2) and their FI (C3, D3 & E3) in all experimental animals (not separated by sex) (C), females (D) and males (E). Asterisks indicate statistically significant effects of the PPS model (*$p < 0.05$, #$0.1 > p > 0.05$). Scale bar 5 μm.

PV+ cells in the lateral geniculate nucleus. Moreover, neurons in the paraventricular nucleus of the thalamus are activated by early life experiences and may contribute to altered susceptibility or resilience to stress during adulthood (Penzo and Gao, 2021). Interestingly, specific changes in the structure and activity of the TRN, namely a reduction in the area of neuronal somata, have been found in rats submitted to maternal separation between P1-P23 (Salas et al., 1986). A similar separation protocol decreased firing frequency and enhanced burst firing in the TRN neurons of young rats (Ali et al., 2013). The studies about the effects of stress during adulthood on the TRN are very scarce, but also point to an important effect of adverse experiences on this inhibitory nucleus. Specifically, chronic restrain stress was shown to induce an increase of PV and WFA immunofluorescence (Pesarico et al., 2019) and to weaken the synaptic strength of the inhibitory input from the TRN to the habenula, which is necessary for the induction of depressive-like behavior (Wang et al., 2023). However, there are studies that have failed to have found effects of acute and chronic stress in the adulthood on GAD65 or GAD67 mRNA expression in the TRN (Bowers et al., 1998).

In this study we have employed a PPS protocol based on psychogenic factors, previously investigated in both male rats (Márquez et al., 2013; Papilloud et al., 2018) and in male and female mice (Bueno-Fernandez

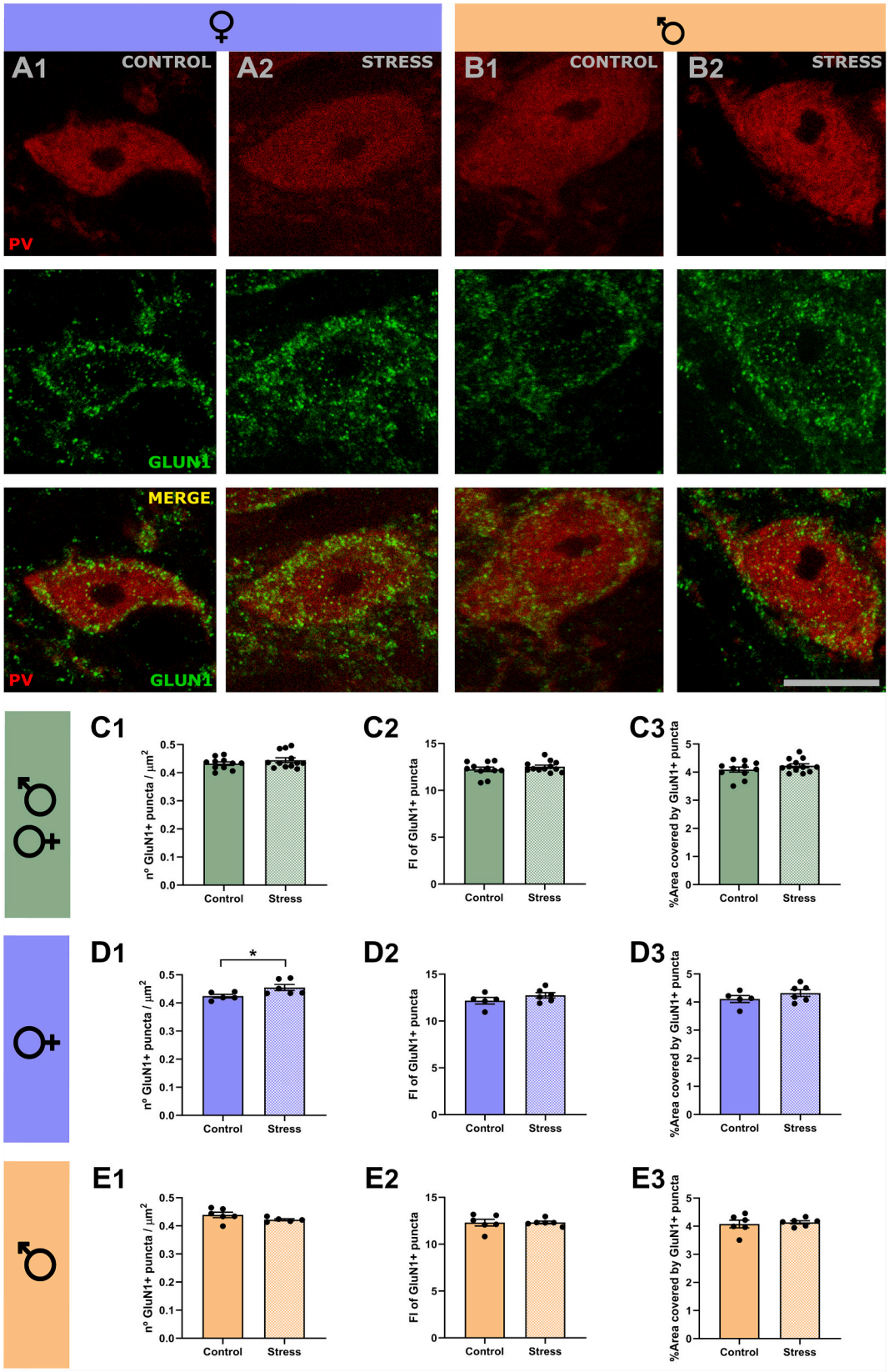

Fig. 7. Effects of the PPS model on the expression of the NMDA receptor subunit 1 (GluN1) in PV+ cells of the TRN. (A-B) Single confocal planes of PV+ cells (red) and GluN1 receptor positive puncta (green) in the TRN of control and stressed female (A) and male (B) mice. Histograms representing the effects of the PPS model on the density (C1, D1 & E1), FI (C2, D2 & E2) and % of area covered (C3, D3 & E3) by GluN1+ puncta in all animals (not separated by sex; C), females (D) and males (E). Asterisks indicate statistically significant effects of the PPS model (*$p < 0.05$). Scale bar 10 µm. (For interpretation of the references to colour in this figure legend, the reader is referred to the web version of this article.)

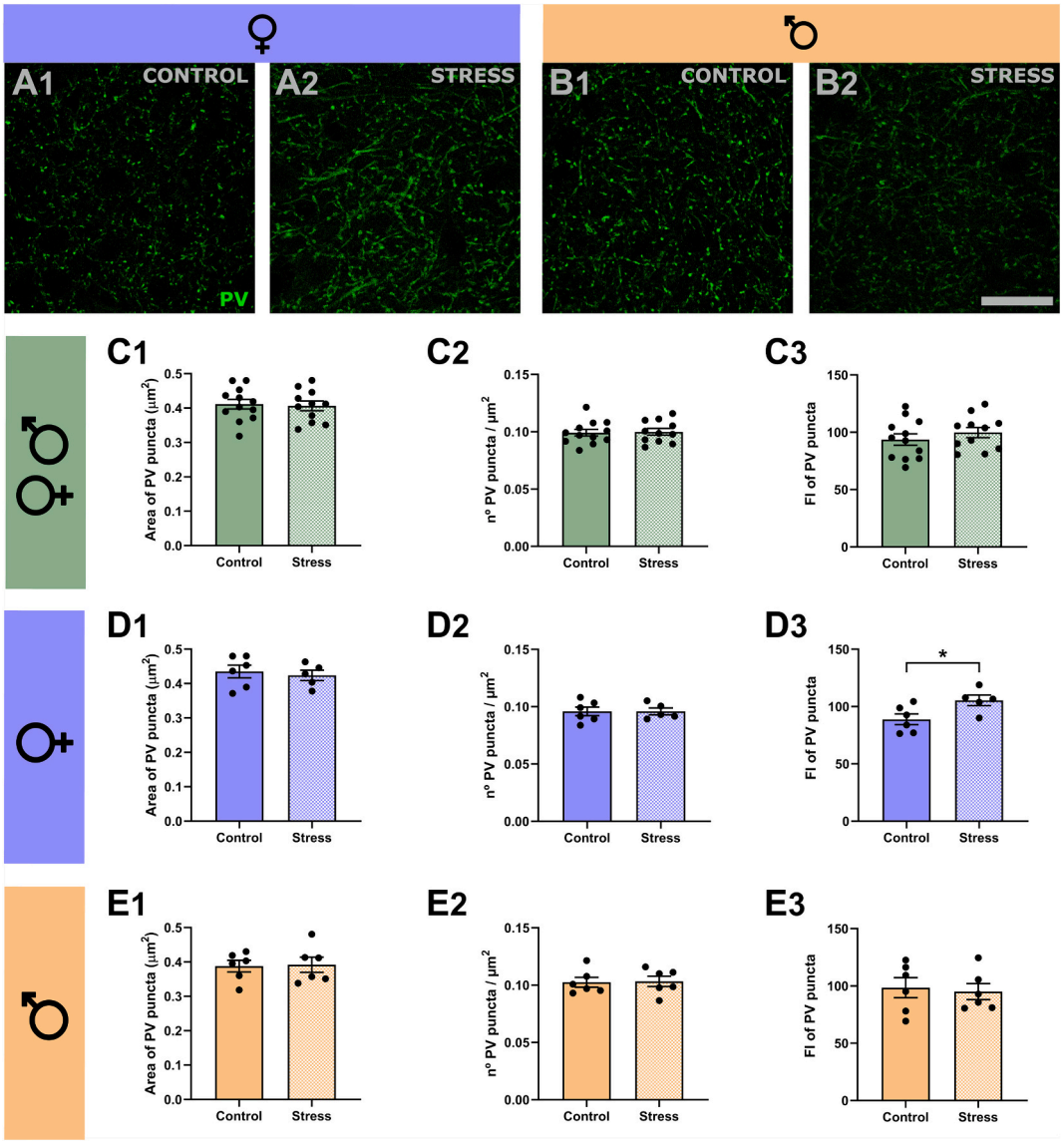

Fig. 8. Study of the effects of the PPS model on the PV immunoreactive puncta in the lateral posterior nucleus (LP). (A-B) Single confocal planes showing PV positive puncta in the LP of females (A) and males (B), comparing control mice (A1, B1) with mice that underwent PPS (A2, B2). Histograms representing differences in the area (C1, D1 & E1), density (C2, D2 & E2) and FI (C3, D3 & E3) of PV immunoreactive puncta in all experimental animals (not separated by sex) (C), females (D) and males (E). Asterisks indicate statistically significant effects of the PPS model (*$p < 0.05$). Scale bar 25 µm.

et al., 2021; Morató et al., 2022). Notably, consistent with findings from our prior study in the medial prefrontal cortex (Bueno-Fernandez et al., 2021), most of the effects in behavior and neuronal structure/connectivity were predominantly detected in females. This observation aligns with the view that females may exhibit a heightened susceptibility to stress-induced disorders (Eid et al., 2019). Using the same PPS protocol, a recent study reported an increased in depressive-like behaviors, as assessed by the open field in adult female mice but not in males (Morató et al., 2022). While our results did not reveal statistically significant differences in this test, there was a trend towards a decrease in some related parameters (Bueno-Fernandez et al., 2021). However, this study identified a significant decrease in the number of licks in the sucrose splash test in females, further indicative of a depressive-like phenotype.

Our volumetric analysis of the TRN also shows reductions only in female mice. This decrease in volume may be due to reductions in the dendritic complexity or in the volume of TRN neurons. In fact, a previous report studying the impact of an earlier adverse experience (maternal separation) in rats reported structural reductions in neuronal somata of the TRN (Salas et al., 1986). Similarly, a single prolonged stress induced bilateral volume reductions in the thalamus of P50 male rats (Yoshii et al., 2017). Interestingly, several studies, including some recent ones, have described volume reductions in the thalamus or specific thalamic nuclei of major depression patients (Amidfar et al., 2021; Chibaatar et al., 2023; Tu et al., 2022). Some of these studies were performed in drug naïve first episode patients and there is a study describing specifically these volumetric reductions in women (Kim et al., 2008). It has to be noted, however, that there are some reports describing contradicting results (Amidfar et al., 2021). Unfortunately, the small size and narrowness of the TRN do not allow the analysis of this nucleus in structural MRI in humans.

The analysis of FosB expression in the PV+ cells of the TRN suggests that PPS does not appear to exert long term effects on the activity of these inhibitory neurons. However, to robustly substantiate this hypothesis, detailed electrophysiological studies are warranted.

Although in general we do not observe significant changes in synaptic puncta in the TRN neuropil, the alterations observed in PNN and PSA-NCAM expression may be indicative of synaptic remodeling in the afferences to this inhibitory nucleus. Previous work has clearly

Table 4
Summary of the Spearman correlations. Table summarizing the results from the Spearman correlations between behavioral analysis and histological studies in the TRN after the PPS model. Asterisks indicate statistically significant effects of the PPS model (#0.10 ≥ p ≥ 0.05, *p < 0.05; **p < 0.01, ***p < 0.001).

		Pooled	Females	Males
Volumetry				
Immobile episodes (PPS mice)	Spearman's rho	−0.088	0.407	−0.786
	p value	0.744	0.317	0.021*
WFA FI in TRN				
Immobile episodes (Control mice)	Spearman's rho	−0.383	−0.738	−0.123
	p value	0.105	0.037*	0.718
N° line crossings (Control mice)	Spearman's rho	0.252	−0.738	−0.37
	p value	0.298	0.037*	0.263
PV/PNN FI ratio				
Immobile episodes (Control mice)	Spearman's rho	0.22	0.905	−0.096
	p value	0.366	0.002**	0.779
N° line crossings (Control mice)	Spearman's rho	−0.396	0.929	−0.005
	p value	0.093#	0.001***	0.989
Density of GLUN1+ puncta				
N° line crossings (Control mice)	Spearman's rho	0.7	0.543	0.9
	p value	0.016*	0.266	0.037*
FI of PV+ puncta in LP				
N° licks total time (PPS mice)	Spearman's rho	0.667	−0.2	−0.928
	p value	0.025*	0.747	0.008**
Periphery distance / center distance (PPS mice)	Spearman's rho	−0.1	−0.9	−0.257
	p value	0.77	0.037*	0.623

demonstrated that both PNN and PSA-NCAM are important regulators of the synaptic input of PV+ interneurons in the cerebral cortex (Carceller et al., 2020; Gómez-Climent et al., 2011). Our results indicate an increase in the complexity of PNN and in their coverage of PV+ interneurons and this may have an impact on the synaptic input of these neurons. This is similar to what we observed in the cerebral cortex, where PNN-covered PV+ cells display more perisomatic synaptic puncta and where the depletion of PNN results in a dramatic loss of inhibitory synaptic puncta (Carceller et al., 2020). In a similar way, the decrease in PSA-NCAM expression in the TRN, may, as in cortical interneurons, augment the area of plasma membrane available for the formation of synaptic inputs (Gómez-Climent et al., 2011; Nacher et al., 2013). Future studies using a more detailed analysis of the synaptic puncta on TRN interneurons, using higher magnification and/or superresolution microscopy, may reveal alterations induced by PPS which are not detected in our current analysis. The remodeling of PNN and PSA-NCAM expression may have an impact on all the inputs received by TRN neurons, but based on the alterations detected in our previous studies in the amygdala and the prefrontal cortex (Bueno-Fernandez et al., 2021; Márquez et al., 2013; Papilloud et al., 2018), we think that direct input from these regions or from the excitatory thalamic nuclei that connect with them (the mediodorsal and LP) would be specially affected. It is interesting to note that the final steps of the maturation of PV+ neurons in the thalamus (Frassoni et al., 1991; Fujita et al., 2022; Majak et al., 1998), as well as the establishment of the adult pattern of their associated PSA-NCAM expression (Mazzetti et al., 2007) and PNN coverage (Vitellaro-Zuccarello et al., 2001) are all processes that are still ongoing during the first 2 months of postnatal life, a period that covers infancy and adolescence in rodents (Brenhouse and Andersen, 2011). Although most of these data have been obtained in rats, unpublished results from our laboratory show that these parameters develop during a similar postnatal time window in mice. We have also studied PV+ puncta in the LP nucleus as a proxy of changes in the synaptic output of TRN cells. The increase in PV immunofluorescence intensity in these puncta may be indicative of a potentiation of this inhibitory input, although further studies are necessary to confirm this hypothesis. In rodents, this nucleus is considered homologous to the pulvinar in primates (Zhou et al., 2017). Interestingly, alterations in the structure, activity and functional connectivity of this nucleus have been described in major depression patients (Hamilton et al., 2012; Li et al., 2022; Xiong et al., 2021).

The physiology of PV+ interneurons is regulated by NMDA receptors (Carlén et al., 2012), which are present in the TRN, particularly enriched in GluN2C and GluN2D subunits (Gawande et al., 2023; Ravikrishnan et al., 2018). As it happens in the present PPS model, the expression of these glutamatergic receptors is altered by chronic stress in the prefrontal cortex (Yuen et al., 2012) and the hippocampus (Sun et al., 2020) of adult male rats. Interestingly, another report described that chronic stress during adolescence did not change GluN1 expression in the hippocampus of female rats, although these animals had a decreased AMPA/NMDA-dependent current ratio compared to controls (Hyer et al., 2021). Our results indicate that PPS changes the expression of NMDA receptors located in PV+ interneurons of the TRN and that this may be important for the alterations in behavior that these animal display during adult life. Analyses of the expression of the different subunits of GluN2, particularly GluN2C and GluN2D in the TRN after chronic stress are warranted in future experiments. It is interesting to note that, although no differences in the expression of any of the NMDA receptor subunits were detected in the thalamus of patients with major depression, they showed reduced levels of SAP102, a PSD protein linked to NMDA receptor-associated signaling (Clinton and Meador-Woodruff, 2004).

The effects of PPS that we have described are likely mediated by glucocorticoid receptors (Papilloud et al., 2019; Veenit et al., 2013). PPS lead to increased corticosterone release during the exposure to stress (Márquez et al., 2013). Glucocorticoid receptors are present in the adult rodent thalamus and, although they are more abundant in the excitatory nuclei, they can be detected in the TRN (Cintra et al., 1994). We have found that these receptors are expressed specifically in PV expressing interneurons in the TRN of young mice, although the expression level was lower than that detected in the principal neurons of the adjacent excitatory nuclei (Supplementary Fig. 1), which is in accordance with previous work describing the expression of glucocorticoid receptor mRNA in the thalamus of early postnatal rats (Yi et al., 1994). However, the actions of glucocorticoids may not be immediate, and it is also possible that the effects of PPS may not be mediated the action of these hormones on their receptors. Consequently, future experiments should perform measurements of glucocorticoid levels and glucocorticoid receptors at different times during the experiment and to block these glucocorticoids to observe whether the effects on TRN were partially or totally dependent on them.

Some papers show evidence of a microglial activation after a prolonged stress in young rodents (Yoshii et al., 2017) and in patients with major depression (Snijders et al., 2021). There is no data on the effects of adverse experiences on thalamic astroglia, although astrocytic dysregulation has been observed in patients with major depression in cortical and subcortical regions (Nagy et al., 2017). However, we have not observed evidence of alterations induced by PPS in the parameters of glial cells studied in our experiment. More detailed analyses on the activation of glial cells, beyond their structural changes, should be performed to detect alterations induced by early life stress.

5. Conclusions

In summary, we present evidence for long-term alterations of behavior and the structure of the TRN in mice subjected to an early life

adverse experience involving psychogenic stressors during adolescence. These changes occur particularly in PV+ inhibitory neurons and molecules associated to their plasticity, such as PSA-NCAM and components of the PNN. Interestingly, most of the effects are observed in female mice and highlight childhood and early adolescence as a time window of higher vulnerability to aversive experiences, especially in female mice.

Supplementary data to this article can be found online at https://doi.org/10.1016/j.nbd.2024.106642.

CRediT authorship contribution statement

Julia Alcaide: Formal analysis, Investigation, Writing – original draft. **Yaiza Gramuntell:** Formal analysis, Investigation. **Patrycja Klimczak:** Formal analysis, Investigation. **Clara Bueno-Fernandez:** Methodology, Investigation. **Erica Garcia-Verellen:** Investigation. **Chiara Guicciardini:** Investigation. **Carmen Sandi:** Conceptualization, Writing – review & editing. **Esther Castillo-Gómez:** Methodology, Investigation. **Carlos Crespo:** Writing – review & editing. **Marta Perez-Rando:** Investigation, Writing – review & editing. **Juan Nacher:** Conceptualization, Writing – review & editing.

Declaration of competing interest

None.

Data availability

Data will be made available on request.

Acknowledgements

This work was supported by the project PID2021-127595OB-I00 and financed by the Spanish Ministry of Science and innovation/AEI/10.13039/501100011033/ ("FEDER Una manera de hacer Europa"), the Generalitat Valenciana (PROMETEU/2020/024) and the Swiss National Science Foundation (No. 31003A_197942); EraNet Neuron Biostress (No. 31NE30_189061). It is also supported by Red Española de Investigación en Estrés/Spanish Network for Stress Research RED2022-134191-T financed by MCIN/AEI /10.13039/501100011033".

References

Alex, A.M., Aguate, F., Botteron, K., Buss, C., Chong, Y.-S., Dager, S.R., Donald, K.A., Entringer, S., Fair, D.A., Fortier, M.V., Gaab, N., Gilmore, J.H., Girault, J.B., Graham, A.M., Groenewold, N.A., Hazlett, H., Lin, W., Meaney, M.J., Piven, J., Qiu, A., Rasmussen, J.M., Roos, A., Schultz, R.T., Skeide, M.A., Stein, D.J., Styner, M., Thompson, P.M., Turesky, T.K., Wadhwa, P.D., Zar, H.J., Zöllei, L., de Los Campos, G., Knickmeyer, R.C., ENIGMA ORIGINs group, 2024. A global multicohort study to map subcortical brain development and cognition in infancy and early childhood. Nat. Neurosci. 27, 176–186. https://doi.org/10.1038/s41593-023-01501-6.

Ali, I., O'Brien, P., Kumar, G., Zheng, T., Jones, N.C., Pinault, D., French, C., Morris, M.J., Salzberg, M.R., O'Brien, T.J., 2013. Enduring effects of early life stress on firing patterns of hippocampal and thalamocortical neurons in rats: implications for limbic epilepsy. PLoS One 8, e66962. https://doi.org/10.1371/journal.pone.0066962.

Amidfar, M., Quevedo, J., Réus, G.Z., Kim, Y.-K., 2021. Grey matter volume abnormalities in the first depressive episode of medication-naïve adult individuals: a systematic review of voxel based morphometric studies. Int. J. Psychiatry Clin. Pract. 25, 407–420. https://doi.org/10.1080/13651501.2020.1861632.

Baker, S.T.E., Lubman, D.I., Yücel, M., Allen, N.B., Whittle, S., Fulcher, B.D., Zalesky, A., Fornito, A., 2015. Developmental changes in brain network hub connectivity in late adolescence. J. Neurosci. 35, 9078–9087. https://doi.org/10.1523/JNEUROSCI.5043-14.2015.

Banasr, M., Duman, R.S., 2008. Glial loss in the prefrontal cortex is sufficient to induce depressive-like behaviors. Biol. Psychiatry 64, 863–870. https://doi.org/10.1016/j.biopsych.2008.06.008.

Banqueri, M., Méndez, M., Arias, J.L., 2018. Why are maternally separated females inflexible? Brain activity pattern of COx and c-Fos. Neurobiol. Learn. Mem. 155, 30–41. https://doi.org/10.1016/j.nlm.2018.06.007.

Banqueri, M., Gutiérrez-Menéndez, A., Méndez, M., Conejo, N.M., Arias, J.L., 2021. Early life stress due to repeated maternal separation alters the working memory acquisition brain functional network. Stress (Amsterdam, Netherlands) 24, 87–95. https://doi.org/10.1080/10253890.2020.1777974.

Bowers, G., Cullinan, W.E., Herman, J.P., 1998. Region-specific regulation of glutamic acid decarboxylase (GAD) mRNA expression in central stress circuits. J. Neurosci. 18, 5938–5947. https://doi.org/10.1523/JNEUROSCI.18-15-05938.1998.

Brenhouse, H.C., Andersen, S.L., 2011. Developmental trajectories during adolescence in males and females: a cross-species understanding of underlying brain changes. Neurosci. Biobehav. Rev. 35, 1687–1703. https://doi.org/10.1016/j.neubiorev.2011.04.013.

Bueno-Fernandez, C., Perez-Rando, M., Alcaide, J., Coviello, S., Sandi, C., Castillo-Gómez, E., Nacher, J., 2021. Long term effects of peripubertal stress on excitatory and inhibitory circuits in the prefrontal cortex of male and female mice. Neurobiol. Stress 14, 100322. https://doi.org/10.1016/j.ynstr.2021.100322.

Cabungcal, J.-H., Steullet, P., Morishita, H., Kraftsik, R., Cuenod, M., Hensch, T.K., Do, K.Q., 2013. Perineuronal nets protect fast-spiking interneurons against oxidative stress. Proc. Natl. Acad. Sci. USA 110, 9130–9135. https://doi.org/10.1073/pnas.1300454110.

Cabungcal, J.-H., Steullet, P., Kraftsik, R., Cuenod, M., Do, K.Q., 2019. A developmental redox dysregulation leads to spatio-temporal deficit of parvalbumin neuron circuitry in a schizophrenia mouse model. Schizophr. Res. 213, 96–106. https://doi.org/10.1016/j.schres.2019.02.017.

Carceller, H., Guirado, R., Ripolles-Campos, E., Teruel-Marti, V., Nacher, J., 2020. Perineuronal nets regulate the inhibitory perisomatic input onto parvalbumin interneurons and γ activity in the prefrontal cortex. J. Neurosci. 40, 5008–5018. https://doi.org/10.1523/JNEUROSCI.0291-20.2020.

Caligioni, C.S., 2009. Assessing reproductive status/stages in mice. Curr. Protoc. Neurosci. https://doi.org/10.1002/0471142301.nsa04is48.

Carceller, H., Gramuntell, Y., Klimczak, P., Nacher, J., 2023. Perineuronal nets: subtle structures with large implications. Neuroscientist 29, 569–590. https://doi.org/10.1177/10738584221106346.

Carlén, M., Meletis, K., Siegle, J.H., Cardin, J.A., Futai, K., Vierling-Claassen, D., Rühlmann, C., Jones, S.R., Deisseroth, K., Sheng, M., Moore, C.I., Tsai, L.-H., 2012. A critical role for NMDA receptors in parvalbumin interneurons for gamma rhythm induction and behavior. Mol. Psychiatry 17, 537–548. https://doi.org/10.1038/mp.2011.31.

Castillo-Gómez, E., Pérez-Rando, M., Bellés, M., Gilabert-Juan, J., Llorens, J.V., Carceller, H., Bueno-Fernández, C., García-Mompó, C., Ripoll-Martínez, B., Curto, Y., Sebastiá-Ortega, N., Moltó, M.D., Sanjuan, J., Nacher, J., 2017. Early social isolation stress and perinatal NMDA receptor antagonist treatment induce changes in the structure and neurochemistry of inhibitory neurons of the adult amygdala and prefrontal cortex. eNeuro 4. https://doi.org/10.1523/ENEURO.0034-17.2017. ENEURO.0034-17.2017.

Cathomas, F., Holt, L.M., Parise, E.M., Liu, J., Murrough, J.W., Casaccia, P., Nestler, E.J., Russo, S.J., 2022. Beyond the neuron: role of non-neuronal cells in stress disorders. Neuron 110, 1116–1138. https://doi.org/10.1016/j.neuron.2022.01.033.

Celio, M.R., Spreafico, R., De Biasi, S., Vitellaro-Zuccarello, L., 1998. Perineuronal nets: past and present. Trends Neurosci. 21, 510–515. https://doi.org/10.1016/s0166-2236(98)01298-3.

Chibaatar, E., Watanabe, K., Okamoto, N., Orkhonselenge, N., Natsuyama, T., Hayakawa, G., Ikenouchi, A., Kakeda, S., Yoshimura, R., 2023. Volumetric assessment of individual thalamic nuclei in patients with drug-naïve, first-episode major depressive disorder. Front. Psychol. 14, 1151551. https://doi.org/10.3389/fpsyt.2023.1151551.

Christian, C.A., Huguenard, J.R., 2013. Astrocytes potentiate GABAergic transmission in the thalamic reticular nucleus via endozepine signaling. Proc. Natl. Acad. Sci. USA 110, 20278–20283. https://doi.org/10.1073/pnas.1318031110.

Cintra, A., Zoli, M., Rosén, L., Agnati, L.F., Okret, S., Wikström, A.C., Gustaffsson, J.A., Fuxe, K., 1994. Mapping and computer assisted morphometry and microdensitometry of glucocorticoid receptor immunoreactive neurons and glial cells in the rat central nervous system. Neuroscience 62, 843–897. https://doi.org/10.1016/0306-4522(94)90481-2.

Clinton, S.M., Meador-Woodruff, J.H., 2004. Abnormalities of the NMDA receptor and associated intracellular molecules in the thalamus in schizophrenia and bipolar disorder. Neuropsychopharmacology 29, 1353–1362. https://doi.org/10.1038/sj.npp.1300451.

Coppola, G., Rurak, G.M., Simard, S., Salmaso, N., 2019. A further analysis and commentary on: profiling changes in cortical astroglial cells following chronic stress. J. Exp. Neurosci. 13 https://doi.org/10.1177/1179069519870182, 1179069519870182.

Cordero, M.I., Rodríguez, J.J., Davies, H.A., Peddie, C.J., Sandi, C., Stewart, M.G., 2005. Chronic restraint stress down-regulates amygdaloid expression of polysialylated neural cell adhesion molecule. Neuroscience 133, 903–910. https://doi.org/10.1016/j.neuroscience.2005.03.046.

De Biasi, S., Amadeo, A., Arcelli, P., Frassoni, C., Meroni, A., Spreafico, R., 1996. Ultrastructural characterization of the postnatal development of the thalamic ventrobasal and reticular nuclei in the rat. Anat. Embryol. (Berl.) 193, 341–353. https://doi.org/10.1007/BF00186691.

Diester, C.M., Banks, M.L., Neigh, G.N., Negus, S.S., 2019. Experimental design and analysis for consideration of sex as a biological variable. Neuropsychopharmacology 44, 2159–2162. https://doi.org/10.1038/s41386-019-0458-9.

Dube, S.R., Felitti, V.J., Dong, M., Giles, W.H., Anda, R.F., 2003. The impact of adverse childhood experiences on health problems: evidence from four birth cohorts dating back to 1900. Prev. Med. 37, 268–277. https://doi.org/10.1016/S0091-7435(03)00123-3.

Eid, R.S., Gobinath, A.R., Galea, L.A.M., 2019. Sex differences in depression: insights from clinical and preclinical studies. Prog. Neurobiol. 176, 86–102. https://doi.org/10.1016/j.pneurobio.2019.01.006.

Eiland, L., Ramroop, J., Hill, M.N., Manley, J., McEwen, B.S., 2012. Chronic juvenile stress produces corticolimbic dendritic architectural remodeling and modulates emotional behavior in male and female rats. Psychoneuroendocrinology 37, 39–47. https://doi.org/10.1016/j.psyneuen.2011.04.015.

Fitzgibbon, T., 2007. Do first order and higher order regions of the thalamic reticular nucleus have different developmental timetables? Exp. Neurol. 204, 339–354. https://doi.org/10.1016/j.expneurol.2006.11.012.

Fogaça, M.V., Duman, R.S., 2019. Cortical GABAergic dysfunction in stress and depression: new insights for therapeutic interventions. Front. Cell. Neurosci. 13, 87. https://doi.org/10.3389/fncel.2019.00087.

Frassoni, C., Bentivoglio, M., Spreafico, R., Sánchez, M.P., Puelles, L., Fairen, A., 1991. Postnatal development of calbindin and parvalbumin immunoreactivity in the thalamus of the rat. Brain Res. Dev. Brain Res. 58, 243–249. https://doi.org/10.1016/0165-3806(91)90011-7.

Fujita, H., Imura, K., Takiguchi, M., Funakoshi, K., 2022. Postnatal development of thalamic reticular nucleus projections to the anterior thalamic nuclei in rats. Eur. J. Histochem. 66, 3370. https://doi.org/10.4081/ejh.2022.3370.

Gawande, D.Y., Shelkar, G.P., Narasimhan, K.K.S., Liu, J., Dravid, S.M., 2023. GluN2D subunit-containing NMDA receptors regulate reticular thalamic neuron function and seizure susceptibility. Neurobiol. Dis. 181, 106117 https://doi.org/10.1016/j.nbd.2023.106117.

Gibel-Russo, R., Benacom, D., Di Nardo, A.A., 2022. Non-cell-autonomous factors implicated in parvalbumin interneuron maturation and critical periods. Front. Neural Circuits 16, 875873. https://doi.org/10.3389/fncir.2022.875873.

Gilabert-Juan, J., Castillo-Gomez, E., Pérez-Rando, M., Moltó, M.D., Nacher, J., 2011. Chronic stress induces changes in the structure of interneurons and in the expression of molecules related to neuronal structural plasticity and inhibitory neurotransmission in the amygdala of adult mice. Exp. Neurol. 232, 33–40. https://doi.org/10.1016/j.expneurol.2011.07.009.

Gilabert-Juan, J., Moltó, M.D., Nacher, J., 2012. Post-weaning social isolation rearing influences the expression of molecules related to inhibitory neurotransmission and structural plasticity in the amygdala of adult rats. Brain Res. 1448, 129–136. https://doi.org/10.1016/j.brainres.2012.01.073.

Gildawie, K.R., Ryll, L.M., Hexter, J.C., Peterzell, S., Valentine, A.A., Brenhouse, H.C., 2021. A two-hit adversity model in developing rats reveals sex-specific impacts on prefrontal cortex structure and behavior. Dev. Cogn. Neurosci. 48, 100924 https://doi.org/10.1016/j.dcn.2021.100924.

Gómez-Climent, M.Á., Guirado, R., Castillo-Gómez, E., Varea, E., Gutierrez-Mecinas, M., Gilabert-Juan, J., García-Mompó, C., Vidueira, S., Sanchez-Mataredona, D., Hernández, S., Blasco-Ibáñez, J.M., Crespo, C., Rutishauser, U., Schachner, M., Nacher, J., 2011. The polysialylated form of the neural cell adhesion molecule (PSA-NCAM) is expressed in a subpopulation of mature cortical interneurons characterized by reduced structural features and connectivity. Cereb. Cortex (New York, N.Y.: 1991) 21, 1028–1041. https://doi.org/10.1093/cercor/bhq177.

Guillery, R.W., Harting, J.K., 2003. Structure and connections of the thalamic reticular nucleus: advancing views over half a century. J. Comp. Neurol. 463, 360–371. https://doi.org/10.1002/cne.10738.

Guirado, R., Carceller, H., Castillo-Gómez, E., Castrén, E., Nacher, J., 2018. Automated analysis of images for molecular quantification in immunohistochemistry. Heliyon 4, e00669. https://doi.org/10.1016/j.heliyon.2018.e00669.

Gundersen, H.J., Jensen, E.B., 1987. The efficiency of systematic sampling in stereology and its prediction. J. Microsc. 147, 229–263. https://doi.org/10.1111/j.1365-2818.1987.tb02837.x.

Hamilton, J.P., Etkin, A., Furman, D.J., Lemus, M.G., Johnson, R.F., Gotlib, I.H., 2012. Functional neuroimaging of major depressive disorder: a meta-analysis and new integration of base line activation and neural response data. Am. J. Psychiatry 169, 693–703. https://doi.org/10.1176/appi.ajp.2012.11071105.

Hansen, K.B., Yi, F., Perszyk, R.E., Menniti, F.S., Traynelis, S.F., 2017. NMDA receptors in the central nervous system. Methods Mol. Biol. (Clifton, NJ) 1677, 1–80. https://doi.org/10.1007/978-1-4939-7321-7_1.

Hensch, T.K., 2005. Critical period plasticity in local cortical circuits. Nat. Rev. Neurosci. 6, 877–888. https://doi.org/10.1038/nrn1787.

Houser, C.R., Vaughn, J.E., Barber, R.P., Roberts, E., 1980. GABA neurons are the major cell type of the nucleus reticularis thalami. Brain Res. 200, 341–354. https://doi.org/10.1016/0006-8993(80)90925-7.

Hu, H., Gan, J., Jonas, P., 2014. Interneurons. Fast-spiking, parvalbumin^{+} GABAergic interneurons: from cellular design to microcircuit function. Science 345, 1255263. https://doi.org/10.1126/science.1255263.

Hyer, M.M., Shaw, G.A., Goswamee, P., Dyer, S.K., Burns, C.M., Soriano, E., Sanchez, C. S., Rowson, S.A., McQuiston, A.R., Neigh, G.N., 2021. Chronic adolescent stress causes sustained impairment of cognitive flexibility and hippocampal synaptic strength in female rats. Neurobiol. Stress 14, 100303. https://doi.org/10.1016/j.ynstr.2021.100303.

Kaiser, T., Ting, J.T., Monteiro, P., Feng, G., 2016. Transgenic labeling of parvalbumin-expressing neurons with tdTomato. Neurosci. 321, 236–245. https://doi.org/10.1016/j.neuroscience.2015.08.036.

Kessler, R.C., Berglund, P., Demler, O., Jin, R., Koretz, D., Merikangas, K.R., Rush, A.J., Walters, E.E., Wang, P.S., National Comorbidity Survey Replication, 2003. The epidemiology of major depressive disorder: results from the National Comorbidity Survey Replication (NCS-R). JAMA 289, 3095–3105. https://doi.org/10.1001/jama.289.23.3095.

Kim, M.J., Hamilton, J.P., Gotlib, I.H., 2008. Reduced caudate gray matter volume in women with major depressive disorder. Psychiatry Res. 164, 114–122. https://doi.org/10.1016/j.pscychresns.2007.12.020.

Klimczak, P., Rizzo, A., Castillo-Gómez, E., Perez-Rando, M., Gramuntell, Y., Beltran, M., Nacher, J., 2021. Parvalbumin interneurons and perineuronal nets in the hippocampus and retrosplenial cortex of adult male mice after early social isolation stress and perinatal NMDA receptor antagonist treatment. Front. Synaptic Neurosci. 13, 733989 https://doi.org/10.3389/fnsyn.2021.733989.

Krol, A., Wimmer, R.D., Halassa, M.M., Feng, G., 2018. Thalamic reticular dysfunction as a circuit endophenotype in neurodevelopmental disorders. Neuron 98, 282–295. https://doi.org/10.1016/j.neuron.2018.03.021.

Li, J., Chen, J., Kong, W., Li, X., Hu, B., 2022. Abnormal core functional connectivity on the pathology of MDD and antidepressant treatment: a systematic review. J. Affect. Disord. 296, 622–634. https://doi.org/10.1016/j.jad.2021.09.074.

Liu, H., Wang, X., Chen, Lu, Chen, Liang, Tsirka, S.E., Ge, S., Xiong, Q., 2021. Microglia modulate stable wakefulness via the thalamic reticular nucleus in mice. Nat. Commun. 12, 4646. https://doi.org/10.1038/s41467-021-24915-x.

Lu, Y., Liang, H., Han, D., Mo, Y., Li, Z., Cheng, Y., Xu, X., Shen, Z., Tan, C., Zhao, W., Zhu, Y., Sun, X., 2016. The volumetric and shape changes of the putamen and thalamus in first episode, untreated major depressive disorder. NeuroImage Clin. 11, 658–666. https://doi.org/10.1016/j.nicl.2016.04.008.

Magdaleno-Madrigal, V.M., Pantoja-Jiménez, C.R., Bazaldúa, A., Fernández-Mas, R., Almazán-Alvarado, S., Bolaños-Alejos, F., Ortíz-López, L., Ramírez-Rodriguez, G.B., 2016. Acute deep brain stimulation in the thalamic reticular nucleus protects against acute stress and modulates initial events of adult hippocampal neurogenesis. Behav. Brain Res. 314, 65–76. https://doi.org/10.1016/j.bbr.2016.07.022.

Majak, K., Berdel, B., Kowiański, P., Dziewiatkowski, J., Lipowska, M., Moryś, J., 1998. Parvalbumin immunoreactivity changes in the thalamic reticular nucleus during the maturation of the rat's brain. Folia Neuropathol. 36, 7–14.

Malave, L., van Dijk, M.T., Anacker, C., 2022. Early life adversity shapes neural circuit function during sensitive postnatal developmental periods. Transl. Psychiatry 12, 306. https://doi.org/10.1038/s41398-022-02092-9.

Márquez, C., Poirier, G.L., Cordero, M.I., Larsen, M.H., Groner, A., Marquis, J., Magistretti, P.J., Trono, D., Sandi, C., 2013. Peripuberty stress leads to abnormal aggression, altered amygdala and orbitofrontal reactivity and increased prefrontal MAOA gene expression. Transl. Psychiatry 3, e216. https://doi.org/10.1038/tp.2012.144.

Mayberg, H.S., 2003. Modulating dysfunctional limbic-cortical circuits in depression: towards development of brain-based algorithms for diagnosis and optimised treatment. Br. Med. Bull. 65, 193–207. https://doi.org/10.1093/bmb/65.1.193.

Mazzetti, S., Ortino, B., Inverardi, F., Frassoni, C., Amadeo, A., 2007. PSA-NCAM in the developing and mature thalamus. Brain Res. Bull. 71, 578–586. https://doi.org/10.1016/j.brainresbull.2006.11.015.

McEwen, B.S., 2016. In pursuit of resilience: stress, epigenetics, and brain plasticity. Ann. N. Y. Acad. Sci. 1373, 56–64. https://doi.org/10.1111/nyas.13020.

McKay, M.T., Kilmartin, L., Meagher, A., Cannon, M., Healy, C., Clarke, M.C., 2022. A revised and extended systematic review and meta-analysis of the relationship between childhood adversity and adult psychiatric disorder. J. Psychiatr. Res. 156, 268–283. https://doi.org/10.1016/j.jpsychires.2022.10.015.

Monyer, H., Burnashev, N., Laurie, D.J., Sakmann, B., Seeburg, P.H., 1994. Developmental and regional expression in the rat brain and functional properties of four NMDA receptors. Neuron 12, 529–540. https://doi.org/10.1016/0896-6273(94)90210-0.

Morató, L., Astori, S., Zalachoras, I., Rodrigues, J., Ghosal, S., Huang, W., Guillot de Suduiraut, I., Grosse, J., Zanoletti, O., Cao, L., Auwerx, J., Sandi, C., 2022. eNAMPT actions through nucleus accumbens NAD+/SIRT1 link increased adiposity with sociability deficits programmed by peripuberty stress. Sci. Adv. 8, eabj9109 https://doi.org/10.1126/sciadv.abj9109.

Murthy, S., Kane, G.A., Katchur, N.J., Lara Mejia, P.S., Obiofuma, G., Buschman, T.J., McEwen, B.S., Gould, E., 2019. Perineuronal nets, inhibitory interneurons, and anxiety-related ventral hippocampal neuronal oscillations are altered by early life adversity. Biol. Psychiatry 85, 1011–1020. https://doi.org/10.1016/j.biopsych.2019.02.021.

Nacher, J., Blasco-Ibáñez, J.M., McEwen, B.S., 2002. Non-granule PSA-NCAM immunoreactive neurons in the rat hippocampus. Brain Res. 930, 1–11. https://doi.org/10.1016/s0006-8993(01)03365-0.

Nacher, J., Guirado, R., Castillo-Gómez, E., 2013. Structural plasticity of interneurons in the adult brain: role of PSA-NCAM and implications for psychiatric disorders. Neurochem. Res. 38, 1122–1133. https://doi.org/10.1007/s11064-013-0977-4.

Nagy, C., Torres-Platas, S.G., Mechawar, N., Turecki, G., 2017. Repression of astrocytic connexins in cortical and subcortical brain regions and prefrontal enrichment of H3K9me3 in depression and suicide. Int. J. Neuropsychopharmacol. 20, 50–57. https://doi.org/10.1093/ijnp/pyw071.

Nestler, E.J., 2015. ΔFosB: a transcriptional regulator of stress and antidepressant responses. Eur. J. Pharmacol. 753, 66–72. https://doi.org/10.1016/j.ejphar.2014.10.034.

Orso, R., Creutzberg, K.C., Lumertz, F.S., Kestering-Ferreira, E., Stocchero, B.A., Perrone, M.K., Begni, V., Grassi-Oliveira, R., Riva, M.A., Viola, T.W., 2023. A systematic review and multilevel meta-analysis of the prenatal and early life stress effects on rodent microglia, astrocyte, and oligodendrocyte density and morphology. Neurosci. Biobehav. Rev. 150, 105202 https://doi.org/10.1016/j.neubiorev.2023.105202.

Papilloud, A., Guillot de Suduiraut, I., Zanoletti, O., Grosse, J., Sandi, C., 2018. Peripubertal stress increases play fighting at adolescence and modulates nucleus accumbens CB1 receptor expression and mitochondrial function in the amygdala. Transl. Psychiatry 8, 156. https://doi.org/10.1038/s41398-018-0215-6.

Papilloud, A., Veenit, V., Tzanoulinou, S., Riccio, O., Zanoletti, O., Guillot de Suduiraut, I., Grosse, J., Sandi, C., 2019. Peripubertal stress-induced heightened aggression: modulation of the glucocorticoid receptor in the central amygdala and normalization by mifepristone treatment. Neuropsychopharmacology 44, 674–682. https://doi.org/10.1038/s41386-018-0110-0.

Penzo, M.A., Gao, C., 2021. The paraventricular nucleus of the thalamus: an integrative node underlying homeostatic behavior. Trends Neurosci. 44, 538–549. https://doi.org/10.1016/j.tins.2021.03.001.
Perez-Rando, M., Carceller, H., Castillo-Gomez, E., Bueno-Fernandez, C., García-Mompó, C., Gilabert-Juan, J., Guirado, R., Pesarico, A.P., Nacher, J., 2022. Impact of stress on inhibitory neuronal circuits, our tribute to Bruce McEwen. Neurobiol. Stress 19, 100460. https://doi.org/10.1016/j.ynstr.2022.100460.
Perlman, G., Tanti, A., Mechawar, N., 2021. Parvalbumin interneuron alterations in stress-related mood disorders: a systematic review. Neurobiol. Stress 15, 100380. https://doi.org/10.1016/j.ynstr.2021.100380.
Pesarico, A.P., Bueno-Fernandez, C., Guirado, R., Gómez-Climent, M.Á., Curto, Y., Carceller, H., Nacher, J., 2019. Chronic stress modulates interneuronal plasticity: effects on PSA-NCAM and perineuronal nets in cortical and extracortical regions. Front. Cell. Neurosci. 13, 197. https://doi.org/10.3389/fncel.2019.00197.
Pinault, D., 2004. The thalamic reticular nucleus: structure, function and concept. Brain Res. Brain Res. Rev. 46, 1–31. https://doi.org/10.1016/j.brainresrev.2004.04.008.
Pizzorusso, T., Medini, P., Berardi, N., Chierzi, S., Fawcett, J.W., Maffei, L., 2002. Reactivation of ocular dominance plasticity in the adult visual cortex. Science 298, 1248–1251. https://doi.org/10.1126/science.1072699.
Ravikrishnan, A., Gandhi, P.J., Shelkar, G.P., Liu, J., Pavuluri, R., Dravid, S.M., 2018. Region-specific expression of NMDA receptor GluN2C subunit in parvalbumin-positive neurons and astrocytes: analysis of GluN2C expression using a novel reporter model. Neuroscience 380, 49–62. https://doi.org/10.1016/j.neuroscience.2018.03.011.
Salas, M., Torrero, C., Pulido, S., 1986. Undernutrition induced by early pup separation delays the development of the thalamic reticular nucleus in rats. Exp. Neurol. 93, 447–455. https://doi.org/10.1016/0014-4886(86)90166-4.
Sandi, C., 2004. Stress, cognitive impairment and cell adhesion molecules. Nat. Rev. Neurosci. 5, 917–930. https://doi.org/10.1038/nrn1555.
Sandi, C., Merino, J.J., Cordero, M.I., Touyarot, K., Venero, C., 2001. Effects of chronic stress on contextual fear conditioning and the hippocampal expression of the neural cell adhesion molecule, its polysialylation, and L1. Neuroscience 102, 329–339. https://doi.org/10.1016/s0306-4522(00)00484-x.
Scheibel, M.E., Scheibel, A.B., 1966. The organization of the nucleus reticularis thalami: a Golgi study. Brain Res. 1, 43–62. https://doi.org/10.1016/0006-8993(66)90104-1.
Schindelin, J., Arganda-Carreras, I., Frise, E., Kaynig, V., Longair, M., Pietzsch, T., Preibisch, S., Rueden, C., Saalfeld, S., Schmid, B., Tinevez, J.-Y., White, D.J., Hartenstein, V., Eliceiri, K., Tomancak, P., Cardona, A., 2012. Fiji: an open-source platform for biological-image analysis. Nat. Methods 9, 676–682. https://doi.org/10.1038/nmeth.2019.
Shaw, G.A., Dupree, J.L., Neigh, G.N., 2020. Adolescent maturation of the prefrontal cortex: role of stress and sex in shaping adult risk for compromise. Genes Brain Behav. 19, e12626 https://doi.org/10.1111/gbb.12626.
Sherman, S.M., 2007. The thalamus is more than just a relay. Curr. Opin. Neurobiol. 17, 417–422. https://doi.org/10.1016/j.conb.2007.07.003.
Snijders, G.J.L.J., Sneeboer, M.A.M., Fernández-Andreu, A., Udine, E., Psychiatric donor program of the Netherlands Brain Bank (NBB-Psy), Boks, M.P., Ormel, P.R., van Berlekom, A.B., van Mierlo, H.C., Böttcher, C., Priller, J., Raj, T., Hol, E.M., Kahn, R. S., de Witte, L.D., 2021. Distinct non-inflammatory signature of microglia in post-mortem brain tissue of patients with major depressive disorder. Mol. Psychiatry 26, 3336–3349. https://doi.org/10.1038/s41380-020-00896-z.
Steullet, P., Cabungcal, J.-H., Bukhari, S.A., Ardelt, M.I., Pantazopoulos, H., Hamati, F., Salt, T.E., Cuenod, M., Do, K.Q., Berretta, S., 2018. The thalamic reticular nucleus in schizophrenia and bipolar disorder: role of parvalbumin-expressing neuron networks and oxidative stress. Mol. Psychiatry 23, 2057–2065. https://doi.org/10.1038/mp.2017.230.
Sun, D.-S., Zhong, G., Cao, H.-X., Hu, Y., Hong, X.-Y., Li, T., Li, X., Liu, Q., Wang, Q., Ke, D., Liu, G.-P., Ma, R.-H., Luo, D.-J., 2020. Repeated restraint stress led to cognitive dysfunction by NMDA receptor-mediated hippocampal CA3 dendritic spine impairments in juvenile Sprague-Dawley rats. Front. Mol. Neurosci. 13, 552787 https://doi.org/10.3389/fnmol.2020.552787.
Takata, N., 2020. Thalamic reticular nucleus in the thalamocortical loop. Neurosci. Res. 156, 32–40. https://doi.org/10.1016/j.neures.2019.12.004.
Tu, P.-C., Chang, W.-C., Chen, M.-H., Hsu, J.-W., Lin, W.-C., Li, C.-T., Su, T.-P., Bai, Y.-M., 2022. Identifying common and distinct subcortical volumetric abnormalities in 3 major psychiatric disorders: a single-site analysis of 640 participants. J. Psychiatry Neurosci. 47, E230–E238. https://doi.org/10.1503/jpn.210154.
Tzanoulinou, S., Sandi, C., 2017. The programming of the social brain by stress during childhood and adolescence: from rodents to humans. Curr. Top. Behav. Neurosci. 30, 411–429. https://doi.org/10.1007/7854_2015_430.
Varea, E., Castillo-Gómez, E., Gómez-Climent, M.A., Blasco-Ibáñez, J.M., Crespo, C., Martínez-Guijarro, F.J., Nàcher, J., 2007. PSA-NCAM expression in the human prefrontal cortex. J. Chem. Neuroanat. 33, 202–209. https://doi.org/10.1016/j.jchemneu.2007.03.006.
Veenit, V., Cordero, M.I., Tzanoulinou, S., Sandi, C., 2013. Increased corticosterone in peripubertal rats leads to long-lasting alterations in social exploration and aggression. Front. Behav. Neurosci. 7, 26. https://doi.org/10.3389/fnbeh.2013.00026.
Velasco, M., Velasco, F., Jiménez, F., Carrillo-Ruiz, J.D., Velasco, A.L., Salín-Pascual, R., 2006. Electrocortical and behavioral responses elicited by acute electrical stimulation of inferior thalamic peduncle and nucleus reticularis thalami in a patient with major depression disorder. Clin. Neurophysiol. 117, 320–327. https://doi.org/10.1016/j.clinph.2005.10.023.
Vitellaro-Zuccarello, L., Meroni, A., Amadeo, A., De Biasi, S., 2001. Chondroitin sulfate proteoglycans in the rat thalamus: expression during postnatal development and correlation with calcium-binding proteins in adults. Cell Tissue Res. 306, 15–26. https://doi.org/10.1007/s004410100425.
Vukadinovic, Z., 2014. NMDA receptor hypofunction and the thalamus in schizophrenia. Physiol. Behav. 131, 156–159. https://doi.org/10.1016/j.physbeh.2014.04.038.
Wang, X.-Y., Xu, X., Chen, R., Jia, W.-B., Xu, P.-F., Liu, X.-Q., Zhang, Ying, Liu, X.-F., Zhang, Yan, 2023. The thalamic reticular nucleus-lateral habenula circuit regulates depressive-like behaviors in chronic stress and chronic pain. Cell Rep. 42, 113170 https://doi.org/10.1016/j.celrep.2023.113170.
Xiong, G., Dong, D., Cheng, C., Jiang, Y., Sun, X., He, J., Li, C., Gao, Y., Zhong, X., Zhao, H., Wang, X., Yao, S., 2021. Potential structural trait markers of depression in the form of alterations in the structures of subcortical nuclei and structural covariance network properties. NeuroImage Clin. 32, 102871 https://doi.org/10.1016/j.nicl.2021.102871.
Yamamuro, K., Yoshino, H., Ogawa, Y., Makinodan, M., Toritsuka, M., Yamashita, M., Corfas, G., Kishimoto, T., 2018. Social isolation during the critical period reduces synaptic and intrinsic excitability of a subtype of pyramidal cell in mouse prefrontal cortex. Cereb. Cortex (New York, N.Y.: 1991) 28, 998–1010. https://doi.org/10.1093/cercor/bhx010.
Yi, S.J., Masters, J.N., Baram, T.Z., 1994. Glucocorticoid receptor mRNA ontogeny in the fetal and postnatal rat forebrain. Mol. Cell. Neurosci. 5, 385–393. https://doi.org/10.1006/mcne.1994.1048.
Yoshii, T., Oishi, N., Ikoma, K., Nishimura, I., Sakai, Y., Matsuda, K., Yamada, S., Tanaka, M., Kawata, M., Narumoto, J., Fukui, K., 2017. Brain atrophy in the visual cortex and thalamus induced by severe stress in animal model. Sci. Rep. 7, 12731. https://doi.org/10.1038/s41598-017-12917-z.
Yuen, E.Y., Wei, J., Liu, W., Zhong, P., Li, X., Yan, Z., 2012. Repeated stress causes cognitive impairment by suppressing glutamate receptor expression and function in prefrontal cortex. Neuron 73, 962–977. https://doi.org/10.1016/j.neuron.2011.12.033.
Zhang, X., Yao, S., Zhu, Xiongzhao, Wang, X., Zhu, Xueling, Zhong, M., 2012. Gray matter volume abnormalities in individuals with cognitive vulnerability to depression: a voxel-based morphometry study. J. Affect. Disord. 136, 443–452. https://doi.org/10.1016/j.jad.2011.11.005.
Zhao, D., Liu, C., Cui, M., Liu, J., Meng, F., Lian, H., Wang, D., Hu, F., Liu, D., Li, C., 2021. The paraventricular thalamus input to central amygdala controls depression-related behaviors. Exp. Neurol. 342, 113744 https://doi.org/10.1016/j.expneurol.2021.113744.
Zhou, N.A., Maire, P.S., Masterson, S.P., Bickford, M.E., 2017. The mouse pulvinar nucleus: organization of the tectorecipient zones. Vis. Neurosci. 34, E011. https://doi.org/10.1017/S0952523817000050.
Zhu, X., Cabungcal, J.-H., Cuenod, M., Uliana, D.L., Do, K.Q., Grace, A.A., 2021. Thalamic reticular nucleus impairments and abnormal prefrontal control of dopamine system in a developmental model of schizophrenia: prevention by N-acetylcysteine. Mol. Psychiatry 26, 7679–7689. https://doi.org/10.1038/s41380-021-01198-8.